Progressive overfilling of readily releasable pool underlies short-term facilitation at recurrent excitatory synapses in layer 2/3 of the rat prefrontal cortex

Jiwoo Shin, Seung Yeon Lee, Yujin Kim ✉ , Suk-Ho Lee ✉

Department of Brain and Cognitive Science, College of Natural Sciences, Seoul National University, Seoul, South Korea • Department of Physiology, Seoul National University College of Medicine, Seoul, South Korea

eLife Assessment

This **valuable** work explores how synaptic activity encodes information during memory tasks. All reviewers agree that the quality of the work is high. Although experimental data do support the possibility that phospholipase diacylglycerol signaling and synaptotagmin 7 (Syt7) dynamically regulate the vesicle pool required for presynaptic release, concerns remain that the central finding of paired pulse depression at very short intervals was more likely caused by Ca2+ channel inactivation than pool depletion. Overall, this is a **solid** study although the results warrant consideration of alternative interpretations.

https://doi.org/10.7554/eLife.102923.1.sa3

Abstract

Short-term facilitation of recurrent excitatory synapses within the cortical network has been proposed to support persistent activity during working memory tasks, yet the underlying mechanisms remain poorly understood. We characterized short-term plasticity at the local excitatory synapses in layer 2/3 of the rat medial prefrontal cortex and studied its presynaptic mechanisms. Low-frequency stimulation induced slowly developing facilitation, whereas high-frequency stimulation initially induced strong depression followed by rapid facilitation. This non-monotonic delayed facilitation after a brief depression resulted from a high vesicular fusion probability and slow activation of Ca^{2+}-dependent vesicle replenishment, which led to the overfilling of release sites beyond their basal occupancy. Pharmacological and gene knockdown (KD) experiments revealed that the facilitation was mediated by phospholipase C/diacylglycerol signaling and synaptotagmin 7 (Syt7). Notably, Syt7 KD abolished facilitation and slowed the refilling rate of vesicles with high fusion probability. Furthermore, Syt7 deficiency in layer 2/3 pyramidal neurons impaired the acquisition of trace fear memory and reduced c-Fos activity. In conclusion, Ca^{2+}- and Syt7-dependent

overfilling of release sites mediates synaptic facilitation at L2/3 recurrent excitatory synapses and contributes to temporal associative learning.

Introduction

Synapses in the mammalian central nervous system undergo activity-dependent modulation of synaptic weight during repetitive stimulation, known as short-term synaptic plasticity (STP). STP is mediated by presynaptic mechanisms that regulate the release probability (p_r), size of the readily releasable pool (RRP), and kinetics of vesicle replenishment of RRP (Zucker and Regehr, 2002; Jackman and Regehr, 2017; Neher and Brose, 2018). Short-term depression has been observed at synapses with a high baseline p_r, primarily because of the rapid depletion of releasable vesicles during high-frequency stimulation (HFS) (Lin et al., 2022). Conversely, vesicle depletion is less pronounced at synapses with a low baseline p_r, and cumulative increases in p_r during HFS are considered to mediate short-term facilitation (Rozov et al., 2001; Pan and Zucker, 2009; Aldahabi et al., 2024). Central synapses exhibit a wide spectrum of STP depending on different combinations of presynaptic factors mediating short-term depression and facilitation.

Previously, facilitation was modeled as an increase in p_r after an action potential (AP) and its slow decay during the inter-spike interval (ISI), resulting in a cumulative increase in p_r during HFS (Markram et al., 1998; Dittman et al., 2000). Recent studies have suggested that the number of docking (or release) sites in an active zone is limited and only partially occupied by releasable vesicles in the resting states (Miki et al., 2016; Pulido and Marty, 2018; Malagon et al., 2020; Lin et al., 2022). Therefore, p_r is determined by the vesicular fusion probability (p_v) and release site occupancy (p_{occ}). However, distinguishing the individual contributions of p_v and p_{occ} to p_r is challenging (Silva et al., 2021; Neher, 2024). It is also unclear whether facilitation is mediated by activity-dependent increases in the p_v, p_{occ}, or both.

Two recent models for vesicle priming and release view the 'priming' as a two-step reversible process that leads to a release-ready state. The release-ready vesicles could be vesicles in a tightly docked state (TS) or those occupying specialized docking sites (DS), and are supplied from vesicles in a loosely docked state (LS) or those occupying a distinct replacement sites (RS), which are called LS/TS model ((Neher, 2024); (Aldahabi et al., 2024)) and RS/DS model ((Miki et al., 2016); (Silva et al., 2021)), respectively. Common to both models is the assumption that release-ready vesicles constitute only a fraction of all docked vesicles under resting conditions and that this fraction is up- and down-regulated by synaptic activity.

Synaptotagmin-7 (Syt7) was recently found to play a crucial role in facilitation at different types of central synapses (Jackman et al., 2016; Chen et al., 2017; Martinetti et al., 2022). In addition to its role in facilitation, Syt7 accelerates refilling of the RRP after depletion and mediates asynchronous release (Bacaj et al., 2013; Liu et al., 2014; Jackman et al., 2016; Tawfik et al., 2021). Syt7-dependent synaptic facilitation is interpreted as an activity-dependent increase in p_v (Turecek et al., 2016; Jackman and Regehr, 2017; Turecek et al., 2017; Norman et al., 2023). However, it is unclear whether Syt7 contributes to facilitation through a Ca^{2+}-dependent increase in p_{occ} (i.e., overfilling). Overfilling has been proposed as a mechanism supporting facilitation at the Drosophila neuromuscular junction (Kobbersmed et al., 2020), yet whether this process also occurs at the mammalian central synapses mediated by Syt7 has not been studied.

Facilitation at recurrent excitatory synapses in cortical recurrent networks may play a crucial role in maintaining working memory (Mongillo et al., 2008; Mongillo et al., 2012; Hansel and Mato, 2013). Although layer 2/3 (L2/3) pyramidal cells (PCs) are highly interconnected and represent task-relevant information during a delay period in working memory tasks (Fujisawa et al., 2008; Ozdemir et al., 2020), most studies on local excitatory recurrent synapses in the neocortex have

focused on layer 5 (L5) exhibiting short-term depression (Reyes and Sakmann, 1999 ☑; Hempel et al., 2000 ☑; Yoon et al., 2020 ☑). Further, the synaptic properties of excitatory synapses in L2/3 remain poorly understood.

In the present study, we found that HFS of local excitatory synapses in L2/3 of the medial prefrontal cortex (mPFC) induced initial strong depression followed by delayed facilitation, whereas low-frequency stimulation induced slow monotonous facilitation. This unique form of STP could be explained by 1) high p_v of RRP vesicles at rest and throughout a train stimulation; 2) the low resting vesicular occupancy of RRP and its activity-dependent increase. These conditions led to delayed facilitation through progressive overfilling of release sites during HFS with high p_v vesicles beyond the resting occupancy. Syt7 knockdown (KD) in L2/3 PCs completely abolished these synaptic enhancements by inhibiting the Ca^{2+}-dependent increase in release site occupancy. Finally, behavioral tests for trace fear conditioning showed that Syt7 KD impaired the acquisition of trace fear memory and reduced c-Fos expression in the mPFC. Collectively, these results support that Ca^{2+}- and Syt7-dependent overfilling of release sites mediates synaptic facilitation at L2/3 recurrent excitatory synapses and contributes to temporal associative learning.

Results

Frequency dependence of STP at local excitatory synapses in L2/3 of the prelimbic cortex

We examined STP profiles at recurrent excitatory synapses between L2/3 PCs and at synapses from L2/3-PCs to fast-spiking interneurons (FSINs) in the prelimbic area of the rat mPFC. The PCs and FSINs were identified based on their distinct intrinsic properties and morphologies (Fig. S1). To stimulate presynaptic PCs, L2/3 PCs were transfected with a plasmid encoding oChIEF using *in utero* electroporation (IUE; **Fig. 1A** ☑; Lee et al., 2024 ☑). Photostimulation of the oChIEF-expressing cell soma at 40 Hz consistently evoked single APs with high fidelity throughout the 600-pulse trains (Fig. S2A-B), which was consistent with little use-dependent inactivation of oChIEF (Lin et al., 2009 ☑; Hass and Glickfeld, 2016 ☑).

Given that IUE transfected approximately 10-20% of L2/3 PCs (**Fig. 1A** ☑), we made a whole-cell patch on a non-transfected L2/3 PC or an FSIN (**Fig. 1C** ☑). To stimulate a minimal number of excitatory axon fibers, EPSCs were evoked using minimal optical stimulation (Fig. S3A; 470 nm, 3-4 μm in radius and 3-5 ms in duration). EPSCs evoked by minimal stimulation were examined to determine the uniformity of the kinetic properties (Fig. S3B-C). Moreover, we reassessed the kinetics of EPSCs during trains *post hoc* to ensure uniformity. EPSCs were evoked by 20-pulse trains at 4 different frequencies (5, 10, 20, and 40 Hz) to cover the range of firing rates of PCs observed *in vivo* during working memory tasks (Baeg et al., 2003 ☑). Excitatory synapses from PCs onto both other PCs and FSINs (PC–PC and PC–FSIN) showed strong (~2-fold enhancement) and lasting (several seconds) short-term facilitation at 20 Hz and lower frequencies (**Fig. 1D-E** ☑). The PC-PC synapses exhibited stronger facilitation than did the PC-FSIN synapses.

Steady-state EPSCs at the PC-PC synapses were not significantly different from 5 to 20 Hz (**Fig. 1F** ☑). Frequency invariance at the PC-PC synapses suggests that Ca^{2+}-dependent synaptic facilitation may counteract vesicle depletion in a frequency-dependent manner (Turecek et al., 2017 ☑; Lin et al., 2022 ☑). Despite facilitation at all frequencies, the paired pulse ratio (PPR) rapidly decreased as the ISI decreased (**Fig. 1G, I** ☑). At 40 Hz stimulation, both PC-PC and PC-FSIN synapses initially underwent strong depression then followed by facilitation in a few stimuli (**Fig. 1Dd, Ed** ☑). Such delayed facilitation after paired pulse depression (PPD) has not been previously observed in central synapses except for a slight increase in EPSC at the cerebellar synapses under artificially depolarized conditions (Pulido and Marty, 2018 ☑).
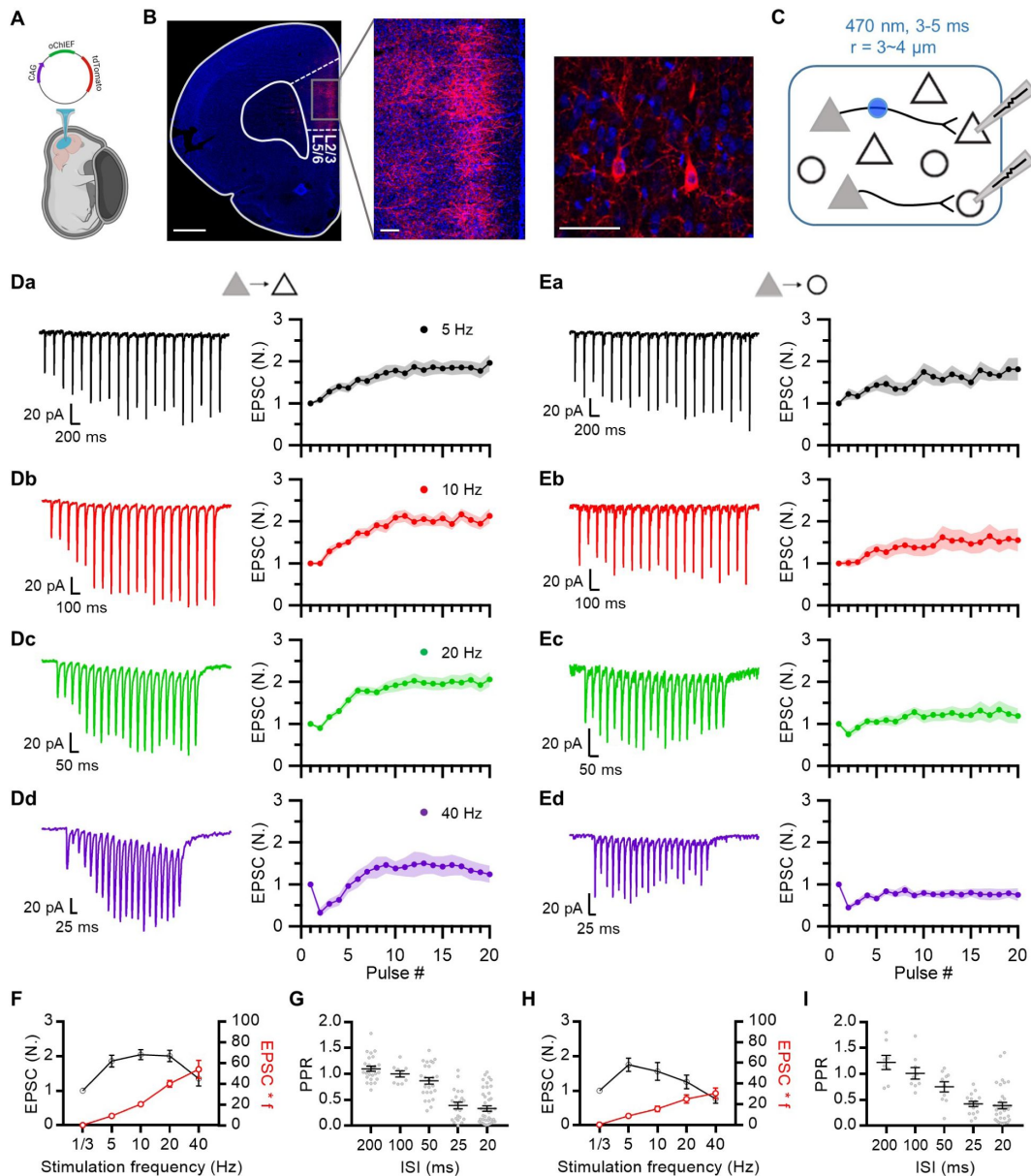
Figure 1.

Frequency-dependence of short-term synaptic plasticity at prelimbic L2/3 excitatory synapses.

(**A**) In utero electroporation following injection of the plasmid (CAG-oChIEF-tdTomato) into the ventricle of an embryo (E17.5). (**B**) Representative images showing specific expression of oChIEF-tdTomato in L2/3 pyramidal cells after IUE. The red fluorescence of tdTomato clearly visualizes oChIEF-expressing cell bodies in L2/3 and axons in L5. Scale bar: 1 mm, 100 µM, 50 µM from left to right. (**C**) Recording schematic showing photostimulation of oChIEF-expressing axon fibers of transfected PCs (*filled triangles*) and a whole-cell recording from non-transfected PCs (*empty triangles*) or FSINs (*empty circles*). A collimated DMD-coupled LED was used to confine the area of excitation (typically 3–4 µm in diameter) to a small region (*blue circle*) near the soma. (**D, E**) Representative traces for EPSCs averaged over 10 trials at each frequency (*left*) and average amplitudes of baseline-normalized EPSCs (*right*) during 20-pulse trains at frequencies from 5 to 40 Hz at PC-PC (*D*; n = 12, 9, 21, 10 cells for 5, 10, 20, 40 Hz, respectively) and PC-FSIN (*E*; n = 8, 9, 10, 10) synapses. Each data point was normalized to the average of the first EPSC. (**F**) Baseline-normalized amplitudes of steady-state EPSCs (EPSC$_{SS}$; *black symbols*) and synaptic efficacy (EPSC$_{SS}$ × *f*; *red symbols*) as a function of stimulation frequency (*f*) at PC–PC synapses. EPSC$_{SS}$ was measured from the average of last 5 EPSCs from the 20-pulse trains (n = 12, 9, 21, 10). (**G**) Paired pulse ratio (PPR) as a function of inter-spike intervals (n = 25, 9, 25, 22, 43 for 200, 100, 50, 25, 20 ms ISI, respectively) at PC-PC synapses. (**H**) EPSC$_{SS}$ and synaptic efficacy at PC-FSIN (n = 8, 9, 10, 10). (**I**) PPR at PC-FSIN (n = 8, 9, 10, 15, 34). *Gray symbols*, individual data.

We confirmed that optically evoked EPSCs were strictly dependent on AP generation (Fig. S4A), suggesting that EPSCs are evoked by optical stimulation of presynaptic axon fibers rather than by direct depolarization of presynaptic boutons. Additionally, dual patch-clamp techniques showed that the STP of optically evoked EPSCs did not differ from the electrically evoked STP of EPSCs at the PC-FSIN synapses (Fig. S4B). Finally, we confirmed that AMPA receptor (AMPAR) desensitization was not responsible for PPD at 40 Hz, ruling out the possible effects of postsynaptic factors on STP (Fig. S5A), and that AMPAR saturation was not significant during facilitation (Fig. S5B).

Delayed facilitation results from slow activation of Ca^{2+}-dependent vesicle replenishment at a constantly high vesicular fusion probability

The strong PPD at 40 Hz suggests a high vesicular fusion probability (p_v) and likely tight coupling of the releasable vesicles to a Ca^{2+} source. To test this hypothesis, we examined the effects of EGTA, a slow calcium chelator, on synaptic transmission at the PC-PC synapses. The baseline EPSC amplitude ($EPSC_1$) was not affected by incubation of the slice in the bath solution containing 50 μM EGTA-AM for longer than 20 min, supporting tight coupling. Moreover, the PPR was decreased to 0.19, and subsequent facilitation slowed but was still distinct (**Fig. 2A-B**). These findings indicate that the initial p_v should be higher than 0.81 considering vesicle recruitment during ISI. The effects of EGTA-AM were confirmed in the same cell by measuring the baseline EPSC and PPR before and after applying EGTA-AM to the bath. $EPSC_1$ remained unchanged, while PPR was reduced by half (Fig. S6).

Notably, the application of EGTA-AM markedly slowed facilitation at 40 Hz (**Fig. 2A,C**). The frequency invariance of steady-state EPSCs (**Fig. 1F**) and the slower facilitation at 40 Hz in the presence of EGTA (**Fig. 2A**) imply a Ca^{2+}-dependent increase in the refilling rate of the RRP and/or an increase in the p_v of reluctant vesicles in light of previous studies (Hosoi et al., 2007 ; Liu et al., 2014 ; Ritzau-Jost et al., 2014 ; Turecek et al., 2016 ; Ritzau-Jost et al., 2018 ; Kusick et al., 2020). Moreover, facilitation was accelerated at higher stimulation frequencies. The plot of the rate constant for the increase in EPSCs (denoted as k_{STF}, the rate constant for the development of short-term facilitation) as a function of the stimulation frequency (f_{stim}) revealed a linear relationship (**Fig. 2C**). k_{STF} in the presence of EGTA-AM was distinctly below this relationship, supporting the Ca^{2+}-dependent acceleration of facilitation.

k_{STF} was also accelerated when the stimulation frequency was increased from 5 Hz to 40 Hz (**Fig. 2D** ; 1.27 ± 0.18/s to 24.27 ± 3.44/s). Notably, the second 40-Hz train stimulation led to strong PPD, followed by accelerated facilitation (**Fig. 2D,E**). The strong PPD suggests that the vesicular fusion probability kept high during the 5-Hz stimulation, arguing against the possibility for an increase in p_v. Both two-step sequential priming models, LS/TS and RS/DS models, are suitable to interpret our data and we will refer to the different populations of vesicles as TS and LS vesicles, respectively (Taschenberger et al., 2016 ; Neher and Brose, 2018 ; Lin et al., 2022 ; Neher, 2024). Within this framework, vesicles are are released from TS with high p_v both in the resting state and during facilitation, and the delayed facilitation is seen as a result of Ca^{2+}-dependent progressive increase in the occupancy of TS vesicles on docking sites.

Release sites have low baseline occupancy and these are increased during facilitation and post-tetanic augmentation

Given that p_v was greater than 0.8, the two-fold increase in EPSC during 20 pulse train stimulations could not be explained by an increase in p_v. Recent studies have shown that vesicle release sites (N) are limited in number and are partially occupied at rest (Miki et al., 2016 ; Pulido and Marty, 2018 ; Malagon et al., 2020 ; Lin et al., 2022). Under such a high p_v, two-fold
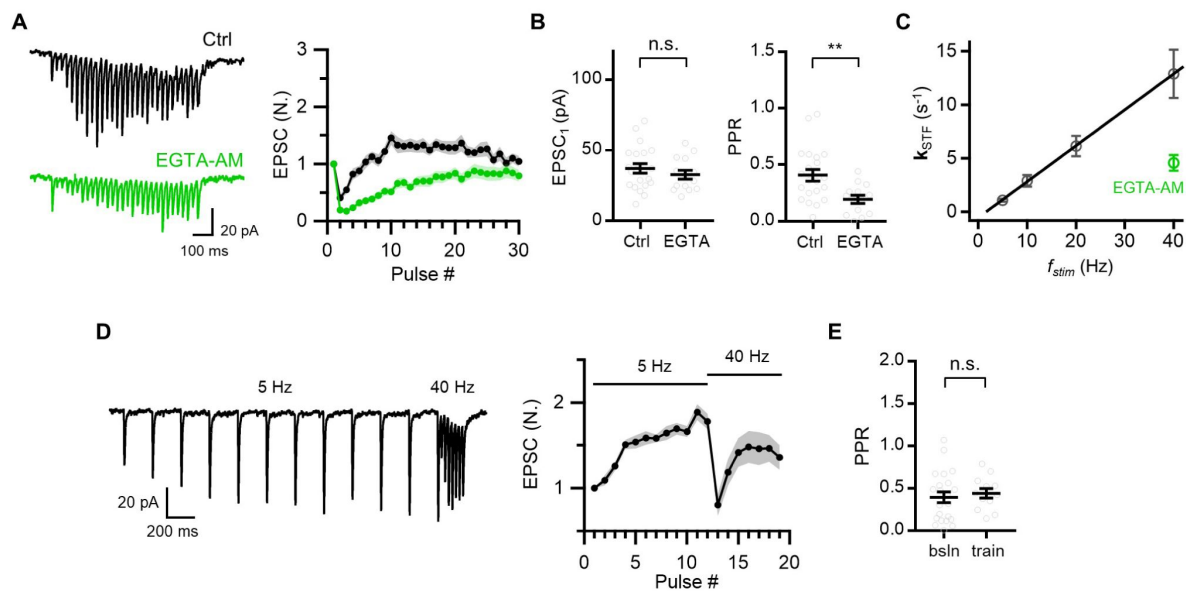
Figure 2.

Delayed facilitation results from slow activation of Ca^{2+}-dependent vesicle replenishment at a constantly high vesicular fusion probability

(**A**) Representative traces (*left*) and mean baseline-normalized amplitudes (*right*) of EPSCs evoked by 30-pulse trains at 40 Hz in control (n = 21; *black*) and in the presence of 50 µM EGTA-AM (n = 14; *green*). (**B**) Mean values for the first EPSC amplitude (EPSC$_1$, *left*) and PPR (*right*) from the experiments displayed in (A). *Gray symbols*, individual data. (**C**) Plot of rate constants for short-term facilitation (k$_{STF}$) as a function of stimulation frequency (f$_{stim}$), showing a linear relationship. The linear regression line (*black*) is shown fitted to k$_{STF}$ values, estimated from **Figure 1** ☑. (**D**) Representative EPSC traces (*left*) and average of baseline-normalized EPSCs (*right*) evoked by 12-pulse stimulation at 5 Hz, followed by 40 Hz 7-pulse train (n = 12). Note that slowly developing facilitation was converted to rapid facilitation after strong PPD. (**E**) Mean values for PPR at 40 Hz. The baseline PPR was reproduced from **Figure 1G** ☑ and the PPR during 5 Hz train was calculated as (13th EPSC) / (12th EPSC). *Gray symbols*, individual data. All statistical data are represented as mean ± S.E.M.; n.s. = not significant; **, P<0.01; unpaired t-test.

synaptic facilitation should be attributed to an increase in p_{occ}. The vesicle replenishment rate is accelerated during HFS in a Ca^{2+}-dependent manner (**Fig.2A-C**⤢; Hosoi et al., 2007⤢). This may lead to the overfilling of release sites beyond their basal vesicular occupancy, which in turn may increase EPSC under high p_v. To test this hypothesis, we determined the quantal parameters at the L2/3 local excitatory synapses. We first measured the quantal size from asynchronous release events after replacing extracellular Ca^{2+} with Sr^{2+}, as previously described (Yoon et al., 2020⤢) (Fig. S7A-B). The mean and coefficient of variance of the quantal sizes were 24 pA and 0.25 at PC-PC synapses, respectively, and were 30 pA and 0.31 at PC-FSIN synapses, (Fig. S7C).

Next, we performed a variance-mean (V-M) analysis of phasic EPSCs at excitatory synapses during train stimulation at 5 Hz and 40 Hz (Scheuss et al., 2002⤢). Applying multiple-probability fluctuation analysis (MPFA) using intra-site quantal variability of 0.2 (Valera et al., 2012⤢), the V-M plot was best fitted by the number of release sites (N) of 5.3 and the quantal size (q) of 25 pA at the PC-PC synapses (**Fig. 3A**⤢). The p_r for $EPSC_1$ was calculated as 0.32. We performed the same analysis for the PC-FSIN synapses and found N = 5.3, q = 35 pA, and p_r for $EPSC_1$ = 0.31 (**Fig. 3B**⤢). Our estimate for N was smaller but comparable to the estimate (6.9) at excitatory synapses in L2/3 of the mouse barrel cortex (Holler et al., 2021⤢).

The p_r estimate was clearly smaller than the possible minimum value for p_v (0.81) estimated from the PPR data (**Fig. 2B**⤢). Given that p_r is a product of p_{occ} and p_v (Neher, 2024⤢), a p_r smaller than p_v indicates the partial occupancy of release sites in the resting state. If synaptic facilitation were mediated by the recruitment of new release sites, it would be accompanied by an increase in the variance of augmented EPSCs (Valera et al., 2012⤢; Kobbersmed et al., 2020⤢). However, the augmented EPSCs during facilitation followed the same parabola in the V-M plot (**Fig. 3A,B**⤢). Therefore, facilitation appears to be mediated by the progressive overfilling of a finite number of release sites beyond the basal occupancy. In the next section, we show that p_v is close to unity based on a synaptic failure analysis (Fig. S8). Assuming this, the baseline p_r at the first pulse estimated from the fitted parabolic curve can be largely regarded as a baseline p_{occ} (c.a. 30%), and the two-fold increase in EPSCs during facilitation can be attributed to an increase of up to 60% in p_{occ}.

We investigated the time course of recovery from facilitation and post-tetanic augmentation (PTA) by applying dual-train stimulations (30 pulses at 40 Hz) separated by different inter-burst intervals (IBIs; **Fig. 3C,D**⤢). The initial EPSCs in the second train were enhanced by more than twofold, and followed by a strong PPD, suggesting that fusion probability stays high in the IBIs and thus synaptic transmission is carried by TS vesicles. The decay time course of PTA was characterized by two phases (initially fast and later slow; **Fig. 3E**⤢), which may reflect a two-phase Ca^{2+} decay or two distinct recovery processes that occur sequentially. The variance of potentiated EPSCs measured at IBIs of 0.1, 0.2, and 0.5 s was not different from that of EPSCs at the peak of facilitation (filled circles, **Fig. 3A-B**⤢). Given that the same RRP mediates both facilitation and augmentation and that post-tetanic EPSCs is carried by TS vesicles similar to the baseline EPSCs, this plot suggests that PTA, similar to short-term facilitation, is mediated by an increase in the TS vesicle occupancy.

Failure rate analysis suggests that vesicular fusion probability is closed to one

The vesicle dynamics of STP has been explained using a simple refilling model (Hosoi et al., 2007⤢; Neher and Sakaba, 2008⤢). This model assumes that the vesicles are reversibly docked to a limited number of release sites (N) with forward and reverse rate constants (denoted as k_1 and b_1, respectively). Under the framework of the simple refilling model (see *Materials and Methods*), the rate constant for the refilling of the RRP after depletion by the first pulse is the sum of the baseline k_1 (k_1) and b_1. This is estimated as 23/s from the plot of PPR as a function of ISIs (Fig. S8A). From the baseline occupancy of 0.3 and $p_{occ} = k_1 / (k_1 + b_1)$, we estimated k_1 to be 6.9/s.
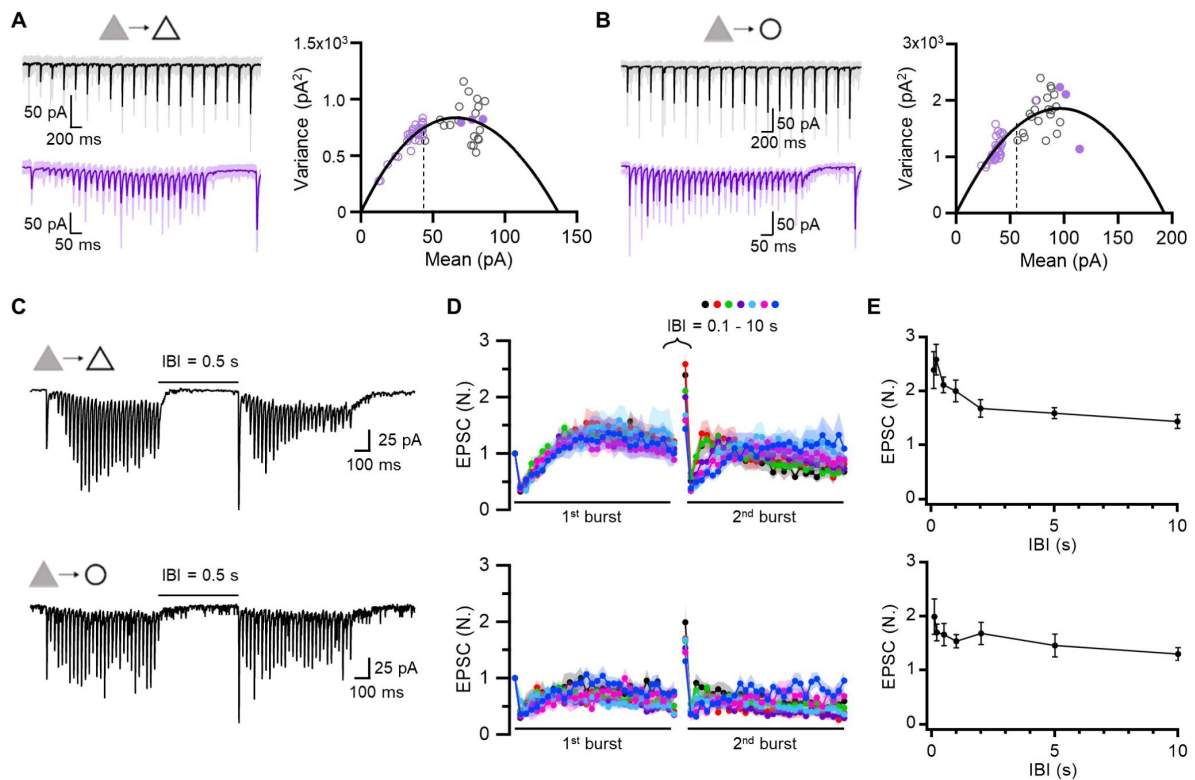
Figure 3.

Low baseline occupancy of release sites and its increase during facilitation and post-tetanic augmentation

(**A, B**) *Left*, Representative EPSCs evoked by 5 and 40 Hz train stimulation (*black*, 5 Hz; *purple*, 40 Hz). *Right*, Variance-mean plots of EPSCs amplitude from averaged EPSCs recorded at PC-PC (A; n = 12, 17 for 5 and 40 Hz, respectively) and PC-FSIN (B; n = 8, 10) synapses. The data were fitted using multiple-probability fluctuation analysis (MPFA). Error bars are omitted for clarity. The 1st EPSC of 5 Hz train (*broken line*) was used to estimate the resting level of p_{occ}. *Filled circles* were measured from post-tetanic augmented EPSCs (*A*, n = 12, 12, 9; *B*, n = 7, 7, 7 for 0.1, 0.2, 0.5 s IBIs, respectively). (**C-E**) Post-tetanic augmentation (PTA) experiments at PC-PC (*top*) and PC-FSIN (*bottom*) synapses. (**C**) Representative traces for EPSCs evoked by double 40 Hz train stimulations separated by 0.5 s. (**D**) Mean baseline-normalized amplitudes of EPSCs evoked by double 40 Hz trains at different inter-burst intervals (IBIs, 0.1, 0.2, 0.5, 1, 2, 5, 10 s). *Upper*, PC-PC synapse (n = 12, 12, 21, 11, 11, 16, 11 from short to long IBIs, respectively). *Lower*, PC-FSIN synapse (n = 10, 9, 8, 9, 9, 7, 9). (**E**) PTA time course. The baseline-normalized amplitudes of 1st EPSC from the 2nd train were plotted as a function of IBIs.

When paired APs were applied with an ISI of 20 ms, the failure rate at 1st pulse, $P(F_1)$, was 10.6%, and the probability of two consecutive failures, $P(F_1, F_2)$, was 6.2% (Fig. S8A). From the equation $P(F_1) = (1 - p_r)^N$, p_r was calculated as 0.312 when N = 6, comparable to p_r (= 0.32) estimated from the V-M analysis (**Fig. 3A**). We calculated $P(F_1, F_2)$ under the framework of a simple refilling model, with p_v and k_1 set as free parameters and other parameters set according to the following relationships: $P(F_1) = (1 - p_r)^N$, $p_r = p_v \cdot p_{occ}$, and $p_{occ} = k_1 / (k_1 + b_1)$.

The calculated values for $P(F_1, F_2)$ and their difference from the observed value (6.2%) are shown in the plane of k_1 *vs.* p_v in Figure S8B-C. As previously mentioned, k_1 was greater than 6/s. Under this high k_1 condition, the difference between the calculated and observed values of $P(F_1,F_2)$ was minimal when $p_v = 1$ (Fig. S8C).

Pharmacological manipulations reveal specific molecular identities underlying vesicle loading processes

Our results suggest that the baseline occupancy of TS vesicles is low and that the activity-dependent progressive overfilling of docking sites with TS vesicles is responsible for short-term facilitation and augmentation. To elucidate the specific molecular link between synaptic enhancement and Ca^{2+}-dependent overfilling, we examined the effects of several drugs known to affect vesicle dynamics. We first examined the roles of phospholipase C (PLC) and diacylglycerol (DAG) by applying 5 μM U73122, a PLC inhibitor, or 20 μM 1-oleoyl-2-acetyl-sn-glycerol (OAG), a DAG analog. The STP at 40 Hz and PTA at 0.5-s interval were examined before and after applying each drug to the bath. For both drugs, the facilitation and augmentation were reduced (**Fig. 4A-B**). U73122 did not affect the basal EPSC amplitude ($EPSC_1$) but resulted in a stronger PPD, slower facilitation, and lower augmentation (**Fig. 4A**). These effects of U73122 suggest the involvement of Ca^{2+}-induced PLC activation in progressive overfilling. In contrast, OAG increased $EPSC_1$ while maintaining a pronounced PPD (**Fig. 4B**), indicating an increase in the TS vesicle pool size. Meanwhile, OAG slowed k_{STF} and reduced augmentation, indicating occlusion of activity-dependent synaptic facilitation. Phorbol esters and DAG are thought to accelerate priming through Munc13 activation (Rhee et al., 2002; Taschenberger et al., 2016; Aldahabi et al., 2022); they also shorten the bridges that interlink docked vesicles with the active zone (AZ) membrane (Papantoniou et al., 2023). Collectively, these suggest that PLC- and DAG-mediated signaling play a role in the overfilling of docking sites underlying short-term facilitation and augmentation.

Although the acceleration of Ca^{2+}-dependent vesicle refilling supports rapid facilitation at 40 Hz, the later part of the delayed facilitation underwent a slight depression, which was more pronounced during the second burst (**Fig. 3D**, **Fig. 4**). Sustained synaptic transmission is limited by the spatial availability of docking sites because it is undermined by accumulation of exocytic remainings in the presynaptic AZ during HFS (Neher, 2010; Haucke et al., 2011). To verify this, we examined the effects of dynasore (100 μM), a specific inhibitor of endocytosis (Macia et al., 2006). The treatment with dynasore did not influence $EPSC_1$ or the early phase of facilitation, but it exacerbated depression during the later phase and attenuated PTA (**Fig. 4C**). This suggests that late synaptic transmission during the 40-Hz train is limited by site clearance.

Given the involvement of actin polymerization in the multiple steps of vesicle docking and recycling, we examined the effects of 20 μM latrunculin B (LatB), an inhibitor of actin polymerization. The effects of LatB were complicated: (1) $EPSC_1$ was decreased, whereas PPR was increased (**Fig. 4Da**) and (2) facilitation and augmentation were reduced (**Fig. 4Db**). The latter effect may result from defects in vesicle replenishment rates, either through the impaired physical movement of vesicles or disrupted site clearance (Sakaba and Neher, 2003; Lee et al., 2012; Hallermann and Silver, 2013; Miki et al., 2016), as Ca^{2+}-dependent vesicle refilling mediates facilitation and augmentation (**Figs. 2**–**3**). Meanwhile, the former effect might be attributed to a shift in equilibrium in the priming states towards a loosely docked state (LS) at rest. It is
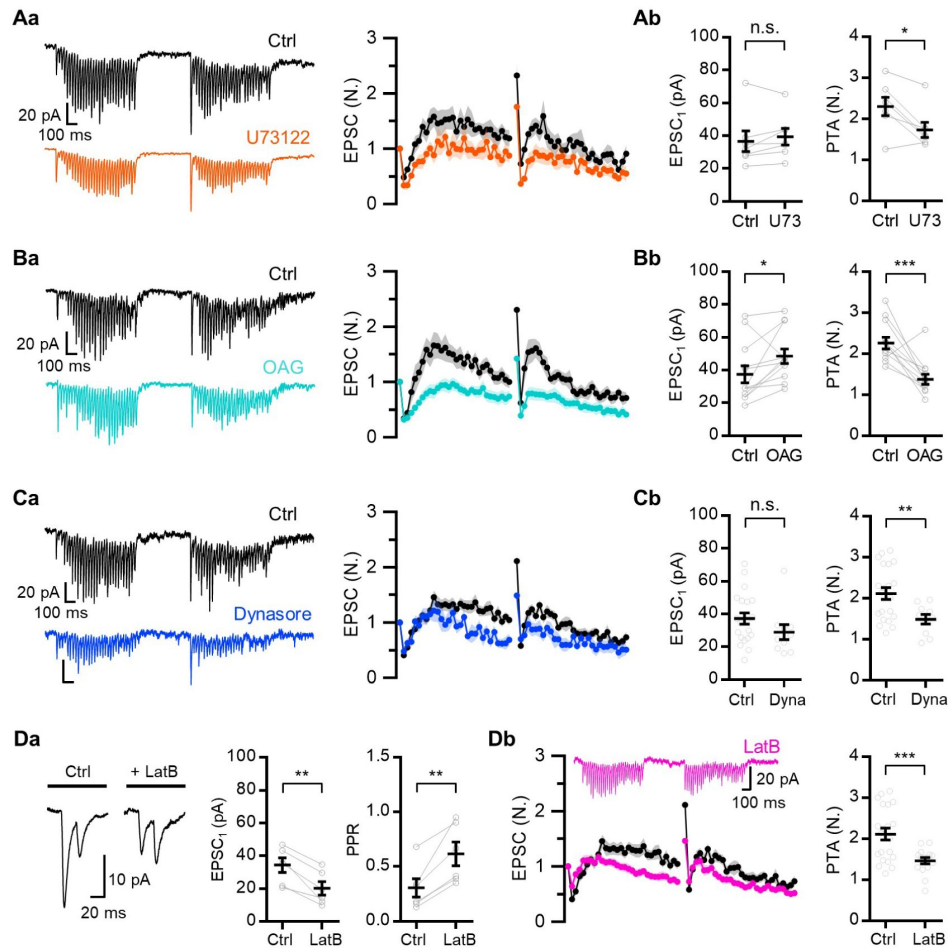
Figure 4.

Pharmacological experiments reveal specific molecular mechanisms underlying vesicle loading processes

(**A-C**) (**a**) Representative EPSC traces (*left*) and mean baseline-normalized EPSCs (*right*) evoked by double 40 Hz train stimulations separated by 0.5 s inter-burst interval (IBI) in control and in the presence of 5 µM U73122 (*Aa*, n = 7, *orange*), 20 µM OAG (*Ba*, n = 12, *cyan*) or 100 µM dynasore (*Ca*, n = 10, *blue*). (**b**) Mean values for baseline EPSCs (EPSC$_1$, *left*) and augmentation (*right*) from the experiments shown in corresponding *a* panel. (**Da**) Representative EPSC traces evoked by paired pulses (*left*) and mean values for baseline EPSC amplitude (*middle*) and PPR (*right*) before and after applying 20 µM LatB (n = 6). (**Db**) Representative EPSC traces (*left, upper*) and average of normalized EPSCs (*left, lower*) evoked by double 40 Hz train stimulation separated by 0.5 s in control (n = 21) and in 20 µM LatB conditions (n = 16; *pink*). *Right*, Mean values for augmentation in control and LatB conditions. *Gray symbols*, individual data. All statistical data are represented as mean ± S.E.M., *, P<0.05; **, P<0.01; ***, P< 0.001; unpaired or paired t-test; n.s. = not significant.

unknown whether actin affects vesicular fusogenicity in neurons, although it facilitates multiple steps of vesicle fusion by enhancing membrane tension in neuroendocrine cells (Wu and Chan, 2022).

Short-term facilitation at both types of local excitatory synapses in L2/3 is abolished by Syt7 knockdown

We examined whether Syt7 mediates facilitation at the PC-PC and PC-FSIN synapses in L2/3 of the mPFC. To this end, oChIEF and shRNA against Syt7 (shSyt7) were co-expressed in L2/3 PCs using IUE. Syt7 KD resulted in a complete loss of facilitation at all tested stimulation frequencies (**Fig. 5A-B**). Short-term depression and paired-pulse depression were more pronounced as the stimulation frequency increased, and the frequency invariance of steady-state EPSC was abolished, implying little contribution of Ca^{2+}-dependent vesicle recruitment (**Fig. 5C-F**). The lack of facilitation could not be attributed to the failure of APs in presynaptic axons, as optical stimulation elicited reliable APs in Syt7 KD PCs during the 40-Hz train (Fig. S2C). Syt7 KD had little effect on the basal properties, including the peak amplitude, rise/decay time, and time-to-peak, of single AP-induced EPSCs (Fig. S3D-E). Moreover, Syt7 KD did not significantly affect the intrinsic properties of neurons (Fig. S9).

To examine whether Syt7 KD had any nonautonomous effects on postsynaptic cells, we measured the quantal size (q) from asynchronous events in the presence of Sr^{2+} and found that the mean quantal size remained unaltered at Syt7 KD synapses (Fig. S7C). This indicated that Syt7 did not influence postsynaptic parameters, including the density and kinetic properties of AMPARs. To test the specificity of shSyt7, we examined whether co-expression of the shRNA-resistant form of Syt7 restored synaptic facilitation in both excitatory synapse types. Presynaptic overexpression of shRNA-resistant Syt7 under the CAG promoter rescued the effect of shRNA at both PC-PC and PC-FSIN synapses (Fig. S10). These results underscore the crucial role of presynaptic Syt7 in mediating short-term facilitation at local excitatory synapses in L2/3 of the mPFC.

Syt7 KD synapses exhibit complementary changes in the number of release sites and their vesicle occupancy

To estimate the quantal parameters in Syt7 KD synapses, we performed V-M analysis of EPSCs evoked by train stimulation (**Fig. 6A-B**). Fitting a parabola to the V-M plot revealed higher baseline p_{occ} in Syt7 KD synapses than in wild-type (WT) synapses for both synapse types (KD, 0.68 and 0.42; WT, 0.32 and 0.31 for PC-PC and PC-FSIN synapses, respectively). The P_{occ} monotonously decreased during a train stimulation, as expected from short-term depression. Moreover, the number of release sites (N) was markedly lower in Syt7 KD synapses (N = 3.5) than in WT synapses (N = 5.3; **Fig. 3A**). Next, we examined the PTA induced by the same protocol as in **Figure 3** (two 40-Hz train stimulations separated by variable IBIs) at Syt7 KD synapses (**Fig. 6C**). The 40 Hz train-induced synaptic depression quickly recovered during IBIs, but no PTA was observed at Syt7 KD synapses, indicating its crucial role in augmentation (**Fig. 6D-E**).

TS vesicle recovery following depletion is accelerated by Syt7

Syt7 is recognized not only for its crucial role in facilitation, but also for mediating Ca^{2+}-dependent replenishment of releasable vesicles (Liu et al., 2014 ; Tawfik et al., 2021). Given that facilitation at L2/3 excitatory synapses is driven by progressive overfilling (**Figs. 2** -**3**), the loss of facilitation at Syt7 KD synapses in the present study implies that Syt7 plays a key role in the Ca^{2+}-dependent acceleration of refilling and overfilling of the docking sites with TS vesicles. To test this hypothesis, we examined the recovery kinetics of EPSCs after TS vesicles were depleted by 3 pulses at 40 Hz in wild-type (WT) and Syt7 KD synapses (**Fig. 7**). Strong PPD was observed not only in the first burst, but also in the second burst. This suggested that EPSCs in the second burst were mediated by TS vesicles, similar to those in the first burst (**Fig. 7A,D**). Therefore, $EPSC_1$ in
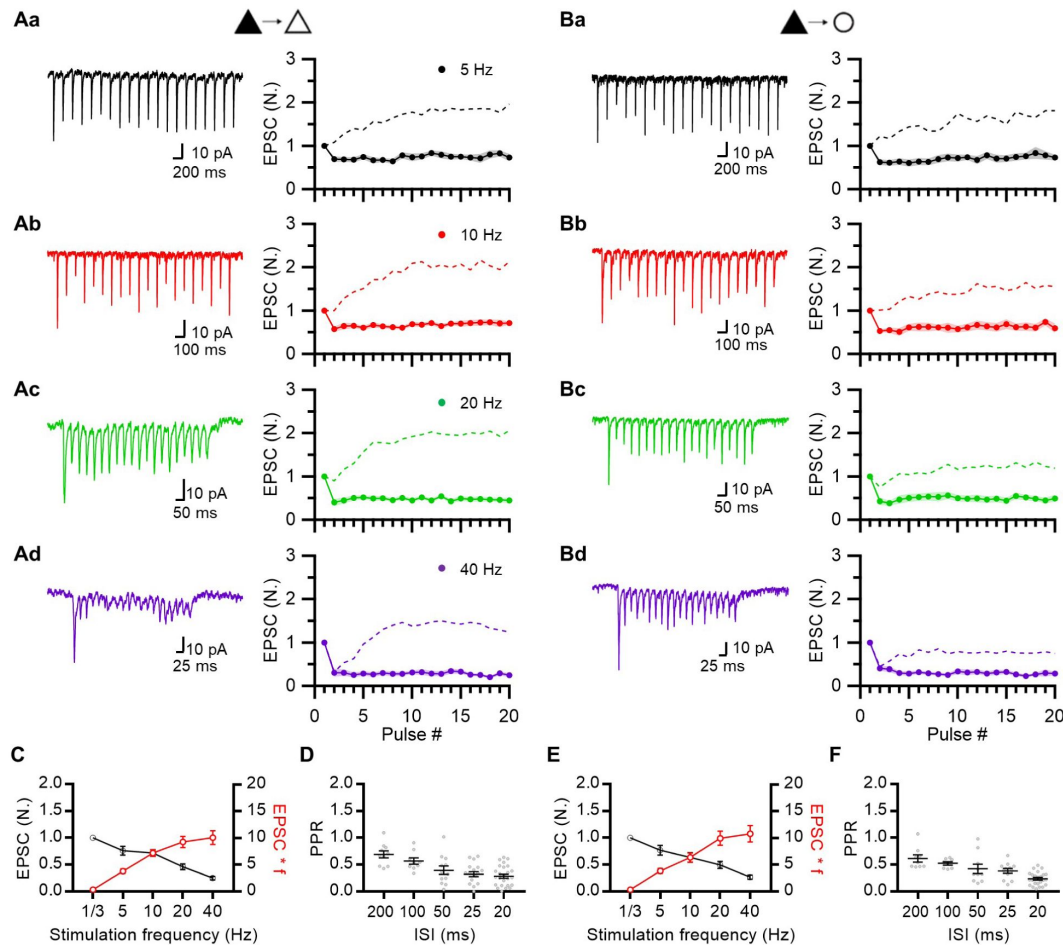
Figure 5.

STF at both types of local excitatory synapses is abolished by Syt7 KD

(**A, B**) Representative EPSC traces (*left*) and mean baseline-normalized amplitudes of EPSCs (*right*) evoked by 20-pulse trains at 5 to 40 Hz. STP was measured at PC-PC (*A*; n = 10, 9, 12, 9) and PC-FSIN (*B*; n = 9, 8, 10, 9) synapses, in which presynaptic Syt7 transcripts were depleted (Syt7 KD). Syt7 KD pyramidal cells are indicated as *black triangles* on the top. For comparison, STP in WT synapses is reproduced from **Figure 1** ☒ (*dotted lines*). Same frequency color codes were used as in **Figure 1** ☒ . (**C**) Baseline-normalized amplitudes of steady-state EPSC (EPSC$_{SS}$; *black symbols*) and synaptic efficacy (EPSC$_{SS}$ × *f*; *red symbols*) as a function of stimulation frequency (*f*) at PC-PC synapses. EPSC$_{SS}$ was defined as the average of last 5 EPSC amplitudes from 20-pulse trains. (**D**) PPR as a function of inter-spike intervals (n = 10, 9, 12, 18, 26). (**E**) EPSC$_{SS}$ and synaptic efficacy at PC-FSIN synapses. (**F**) PPR at PC-FSIN synapses (n = 9, 8, 10, 12, 24). *Gray symbols*, individual data.
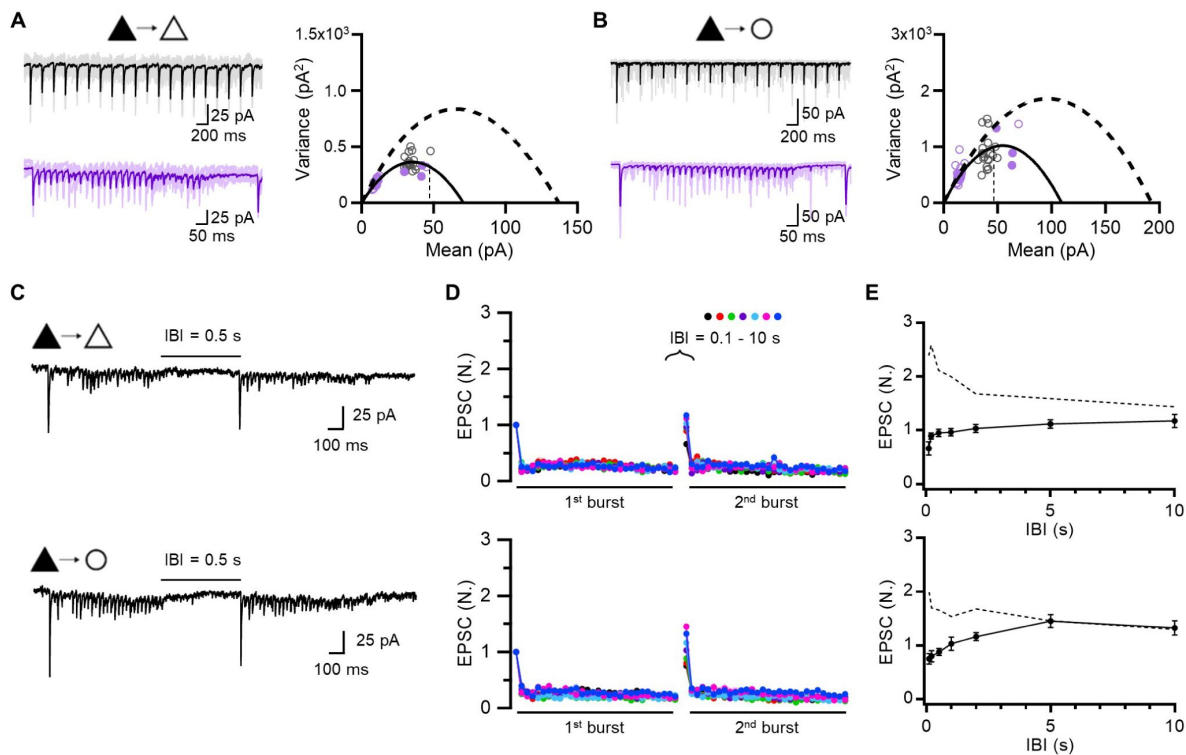
Figure 6.

**Syt7 KD synapses exhibit complementary changes in
the number of release sites and their vesicle occupancy**

(**A, B**) *Left*, Representative traces of EPSCs evoked by 5 and 40 Hz train stimulations (*black*, 5 Hz; *purple*, 40 Hz). *Right*, Variance-mean plots of EPSCs amplitude from averaged EPSCs recorded at PC-PC (*A*; n = 9, 15, 12, 10, 9) and PC-FSIN (*B*; n = 4, 14, 10, 9, 8) synapses in which presynaptic Syt7 has been knocked down. The data were fitted using MPFA and error bars are omitted for clarity. The mean 1st EPSC amplitude of 5 Hz train (*dotted line*) was used for estimation of baseline p_{occ}. *Broken lines* indicate MPFA fits to variance-mean plot of WT synapses reproduced from **Figure 2** . (**C-E**) Recovery experiments at PC-PC (*top*) and PC-FSIN (*bottom*) synapses in which presynaptic Syt7 was knocked-down. (**C**) Representative EPSCs evoked by double 40 Hz train stimulations separated by 0.5 s. (**D**) Mean baseline-normalized amplitudes of EPSCs evoked by double 40 Hz trains at PC-PC (n = 12, 10, 9, 9, 10, 9, 8) and PC-FSIN (n = 10, 9, 10, 11, 8, 9, 10) synapses at different interburst intervals (IBIs). (**E**) PTA time course. Baseline-normalized amplitudes of 1st EPSC from the 2nd burst were plotted as a function of various IBIs. *Dotted lines* indicate augmented EPSCs in the WT reproduced from **Figure 2** .

the second burst can be interpreted as a release from TS vesicles recovering during a given IBI. The recovery time course of $EPSC_1$ in the second burst indicated full recovery of TS vesicles within 100 ms in both excitatory synapse types in WT rats (**Fig. 7C,F**). However, this recovery was remarkably slower in Syt7 KD synapses, requiring 5 s for full recovery, indicating that TS vesicle recovery was greatly accelerated by Syt7. Overall, synaptic facilitation and augmentation at local excitatory synapses in L2/3 can be ascribed to progressive activity-dependent increases in the occupancy of TS vesicles (**Figs. 2**-**3**), in which Syt7 plays a key role.

Behavioral consequences of Syt7 KD in L2/3 PCs of the mPFC

We previously proposed that the disparity in STP between the PC-PC and PC-IN synapses results in activity-dependent changes in the ratio of synaptic weights at the PC-PC and PC-IN synapses (J_{ee}/J_{ie}). This may in turn have a profound influence on persistent activity in a recurrent network by biasing the E-I balance (Yoon et al., 2020). Syt7 KD not only eliminated facilitation, but also the activity-dependent increase in the J_{ee}/J_{ie} ratio in the L2/3 network (Fig. S11). This suggests the possibility that Syt7 contributes to the persistent activity during working memory tasks in the L2/3 recurrent network. Trace fear conditioning (tFC) requires associative learning between an auditory cue (conditioned stimulus, CS) and temporally separate aversive events (unconditioned stimulus, US). The formation of trace fear memory requires the prelimbic area of the mPFC and hippocampus. mPFC activity during the trace interval is thought to temporarily hold CS information, enabling the network to associate temporally discontinuous events (i.e., temporal associative learning) (Gilmartin et al., 2013). Synaptic facilitation and augmentation are implicated in temporary memory retention in recurrent networks (Mongillo et al., 2008; Mongillo et al., 2012).

Given that Syt7 is crucial for synaptic facilitation (**Fig. 5**) and augmentation (**Fig. 6**) in prelimbic L2/3 recurrent excitatory synapses, we tested whether trace fear memory formation was impaired in rats with depleted Syt7 transcripts, specifically in the L2/3 PCs of the mPFC. Syt7-targeted shRNA (shSyt7) or scrambled shRNA (Scr) constructs were transfected bilaterally into the L2/3 PCs of the mPFC using IUE (**Fig. 8A**). Both the Scr-transfected control and shSyt7-transfected rats underwent tFC training (**Fig. 8B**). The following day, the rats were subjected to a tone test in which trace fear memory formation was assessed from the freezing response to a tone alone in a distinct context. Compared to the control group, the shSyt7-transfected group exhibited significantly lower levels of freezing behavior in response to auditory cues during the first four trials, suggesting an impairment in trace memory formation (**Fig. 8C**).

The tone test was repeated the following day to test for extinction memory formation. Syt7 KD animals exhibited much less freezing to the CS (+1d) than did WT animals. Considering the Rescorla-Wagner model (Yau and McNally, 2023), our results suggest that the strength of CS-US associative memory was weaker in KD animals than in WT animals; thus, the acquisition of trace fear memory was impaired by Syt7 KD in the L2/3 PCs of the mPFC.

Next, we assessed the locomotor activity and anxiety levels of rats using the open field test (OFT) and elevated plus maze test (EPM). Scr controls and Syt7 KD rats showed similar exploratory patterns, displaying comparable total distance moved and time spent in the periphery of the OFT or the open/closed arms of the EPM (Fig. S12). Previous studies have suggested that the acquisition of trace fear memory requires elevated trace activity in prelimbic PCs (Gilmartin et al., 2013). Given that c-Fos, an immediate early gene, is upregulated following patterned activities in neurons, its expression is considered a reliable indicator of recent neuronal activation (Fields et al., 1997; Guzowski et al., 2005). To investigate the effect of Syt7 on neuronal activity *in vivo* during tFC, animals were sacrificed at the time of peak c-Fos protein expression, approximately 90 min after completion of the behavioral task (Arime and Akiyama, 2017).
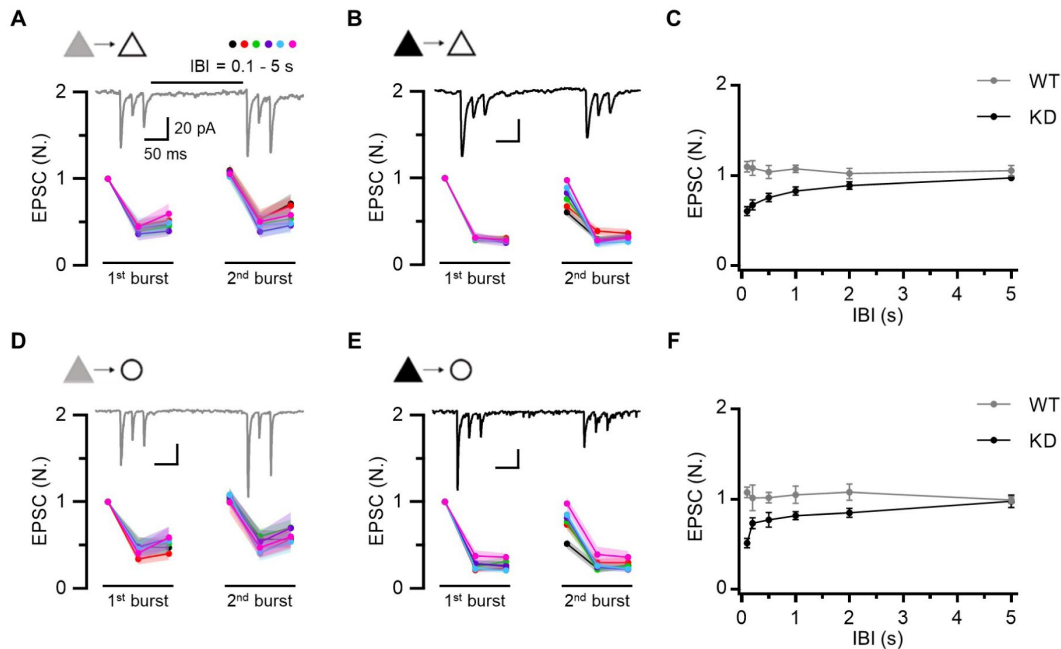
Figure 7.

Recovery of TS vesicles following depletion is accelerated by Syt7

(**A-C**). Recovery experiments at PC-PC synapses in WT (*A*) and Syt7 KD (*B*). Mean baseline-normalized amplitudes of EPSCs evoked by two consecutive 3-pulse 40 Hz trains in WT (n = 16, 13, 11, 11, 11, 9 from short to long IBIs, respectively) and KD (n = 13, 11, 12, 8, 10, 11) synapses at different IBIs (0.1, 0.2, 0.5, 1, 2, 5 s). *Inset*, representative traces of EPSCs evoked by two consecutive 3-pulse 40 Hz train stimulations separated by 0.5 s. (**D-F**). Recovery experiments at PC-FSIN synapses in WT (*D*) and Syt7 KD (*E*). Mean baseline-normalized amplitudes of EPSCs evoked by two consecutive 3-pulse 40 Hz trains in WT (n = 9, 11, 11, 9, 10, 13) and KD (n = 9, 12, 9, 7, 10, 9) synapses at different IBIs. *Inset*, representative traces of EPSCs evoked by two consecutive 3-pulse 40 Hz train stimulations separated by 0.5 s. (**C, F**) Recovery time course. Baseline-normalized amplitudes of 1st EPSC from the 2nd burst were plotted as a function of various IBIs.
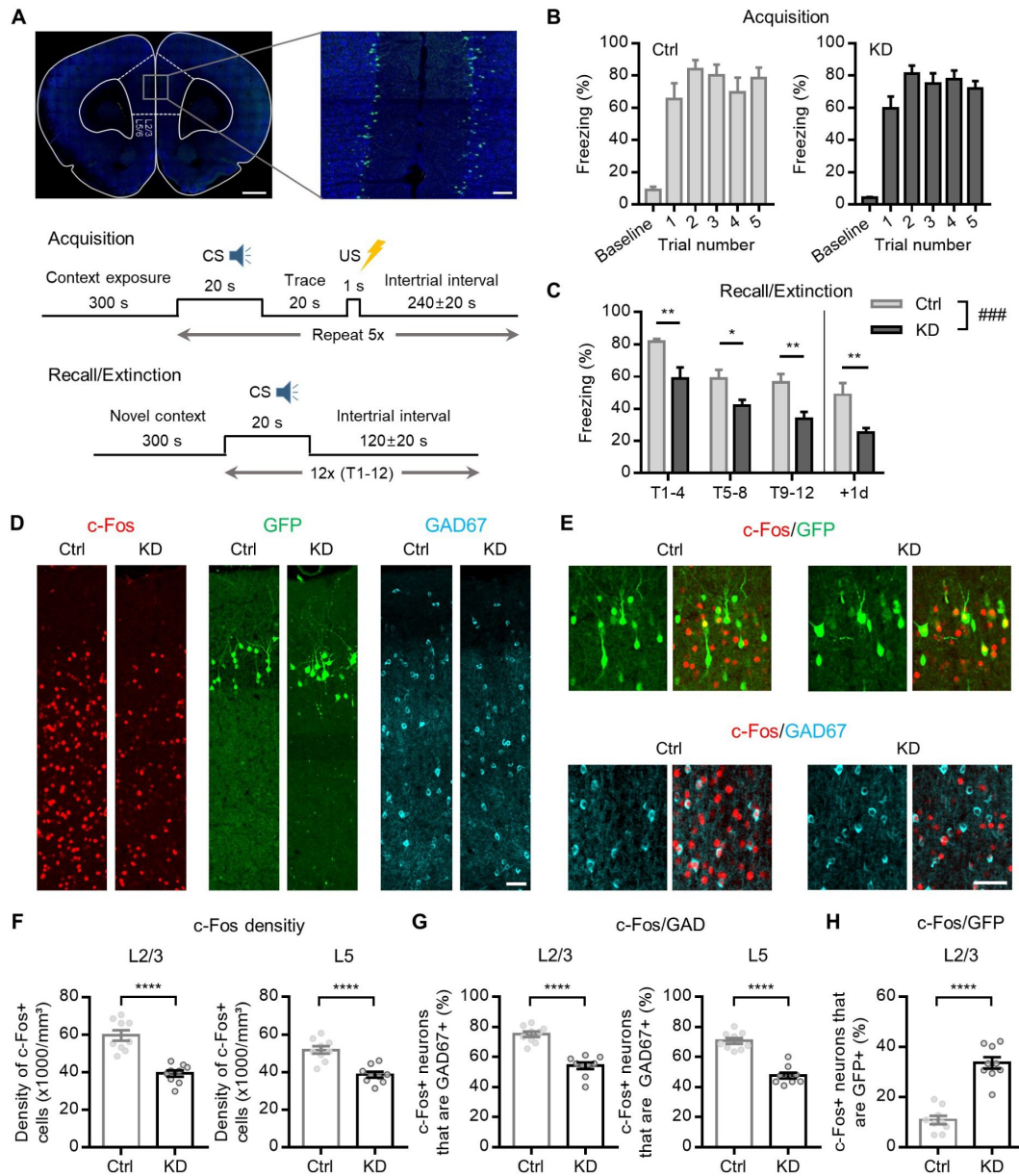
Figure 8.

Behavioral effects of Syt7 deficiency in L2/3 PCs of the mPFC

(**A**) *Top*, Representative images showing bilateral expression of U6-GFP in L2/3 of PCs after IUE at E17.5. Scale bar: 1 mm, 100 μm. *Bottom*, Schematic of trace fear conditioning and extinction (tone test) protocol. (**B**) Freezing behavior of control (expressing scrambled shRNA, *Scr*) and Syt7 KD rats during acquisition of tFC. (**C**) Freezing ratio during tone tests on following days. Data are shown as average freezing during T1–T4, T5–T8, or T9–T12 (T, trials). The freezing on T1-T4 was significantly lower in KD rats suggesting that formation of trace memory was impaired in Syt7 KD rats (n = 10, 11 for Ctrl and KD, respectively; P = 0.0007, F(1, 19) = 16.43, two-way repeated measures ANOVA; P = 0.0064, 0.0211, 0.0064, 0.0064; Holm-Sidak test). (**D**) Representative images of c-Fos immunoreactivity in the prelimbic cortex of control or Syt7 KD rats 90 min after tFC acquisition. c-Fos (*left*, *red*, Cy5) and GAD67 (*right*, *cyan*, Cy3) were immunostained in the same brain slice expressing U6-GFP (*middle*; *green*). Scale bar, 50 μm. (**E**) Exemplar images of c-Fos positive neurons expressing GFP (*top*) or GAD67 (*bottom*) in control (*left*) or Syt7 KD rats (*right*). Scale bar, 50 μm. (**F-H**) Effects of Syt7 KD on c-Fos density (*F*) and percentage of c-Fos positive neurons co-labeled with GAD67 (*G*) or GFP (*H*) in L2/3 or L5 of prelimbic cortex (n = 9, 9 for Ctrl and KD, respectively). *Open symbols*, individual data. All statistical data are represented as mean ± S.E.M.; ****, P<0.0001; unpaired t-test.

To elucidate the activation patterns of specific neuronal populations, we performed immunohistochemical co-labeling of c-Fos and GAD67 (a GABAergic interneuron marker) upon tFC acquisition. The density of c-Fos(+) cells and the percentage of GAD67(+) cells among c-Fos(+) cells in all prelimbic layers were significantly lower in Syt7 KD rats than in control rats (**Fig. 8F-G**). Additionally, analysis of the proportion of active cells among transfected L2/3 PCs (c-Fos+/GFP+) revealed that Syt7 KD L2/3 PCs were significantly more active than Scr-transfected PCs (**Fig. 8H**). This unexpected hyperactivity of Syt7 KD PCs may be attributed to the high reciprocal connectivity between PCs and FSINs in the neocortex (Holmgren et al., 2003; Otsuka and Kawaguchi, 2009), as PCs with short-term depression would transmit less input to FSINs, which in turn would exert less feedback inhibition on reciprocally connected PCs. Collectively, these findings show that the slow activation of vesicle refilling supports various forms of facilitation at excitatory synapses in PFC L2/3, which is essential for neuronal activity during temporal associative learning.

Discussion

The present study characterized STP at local excitatory synapses in the L2/3 network of the rat mPFC at physiological extracellular [Ca^{2+}]. These synapses displayed initial strong depression and then delayed facilitation at 40 Hz, while monotonous slowly developing facilitation was observed at lower frequencies. Our study suggests that such delayed facilitation after a brief depression results from a high p_V (**Figs. 2-3** and Fig. S8), along with Ca^{2+}-dependent delayed acceleration of vesicle refilling and overfilling (**Figs. 2–3**). The two-fold increase in EPSC during 20 pulse train stimulations under the condition of such a high p_V suggests a Ca^{2+}-dependent increase in the vesicle replenishment rate during a train; this then leads to overfilling of release sites beyond their incomplete basal occupancy (**Fig. 3A,B**). The high p_V and strong PPD did not result from artificial bouton stimulation, AMPAR desensitization, or any potential distortion caused by optogenetic methods (Figs. S4 and S5). Additionally, similar to short-term facilitation, PTA could be explained by an increase in the TS vesicle occupancy (**Fig. 3C-E**), consistent with previous studies showing post-tetanic increases in the p_{occ} and/or vesicle pool size at various types of synapses (Lee et al., 2010; Vandael et al., 2020; Tran et al., 2023; Silva et al., 2024). These findings suggest that release sites are partially occupied at rest and that a progressive overfilling of release sites with TS vesicles underlies facilitation and augmentation at intracortical L2/3 excitatory synapses.

Progressive overfilling of docking sites

Conventional models for facilitation assume an increase in p_V after an AP of RRP vesicles, which had been in a low_p_V or reluctant state at rest (Dittman et al., 2000; Turecek et al., 2016). This facilitation model is unlikely to explain our results, because TS vesicles are predominantly released not only at rest but also in the facilitated state during or after train stimulation, as evidenced by the strong PPD (ISI, 25 ms) during a 5-Hz train (**Fig. 2D-E**) and at different intervals after a 40-Hz/30 pulse trains (**Fig. 3D**). Moreover, the PPD (ISI, 25 ms) remained pronounced during the early phase of facilitation (**Fig. 7**), arguing against the possibility of slowly increasing the p_V of reluctant vesicles. These results suggested that facilitation was mediated by an activity-dependent progressive increase in occupancy of TS vesicles (TS occupancy). Facilitation through an increase in TS occupancy has been termed frequency facilitation, differentiating it from paired pulse facilitation that relies on a residual calcium-dependent transient increase in the p_V of releasable vesicles (Neher, 2024).

Assuming an increase in TS occupancy, to attain a two-fold increase in EPSC (**Fig. 1**), the baseline occupancy of the docking sites by TS vesicles should be low, as estimated from the V-M plot (c.a. 30% in **Fig. 3**). However, it is unclear whether the remaining docking sites that are not occupied by TS vesicles are truly vacant or are occupied by reluctant LS vesicles that are not released by the AP or AP trains. TS vesicles can be supplied by the transformation of LS to TS

vesicles, both of which reside at the same docking site (LS/TS model; reviewed in Neher, 2024 ☒). Alternatively, TS vesicles can be supplied from a distinct replacement pool (RS/DS model; reviewed in Silva et al., 2021 ☒). Further studies, including ultrastructural analyses of active zones, are required to address this issue.

Given the crucial role of Syt7 in facilitation (**Fig. 5** ☒), the facilitation mechanisms are closely related to how Syt7 mediates synaptic facilitation. Based on the slow kinetics of Syt7, previous computational modeling studies have proposed that Syt7 may mediate short-term facilitation through an activity-dependent increase in p_v (Turecek et al., 2016 ☒; Jackman and Regehr, 2017 ☒; Turecek et al., 2017 ☒; Norman et al., 2023). The present study, however, found that both facilitation and augmentation were mediated by overfilling of the release sites (**Figs. 2** ☒–**3** ☒). Moreover, Syt7-KD synapses displayed slower recovery of TS vesicles (**Fig. 7** ☒). These results suggest that Syt7 is essential for activity-dependent overfilling of docking sites with TS vesicles. Whereas the baseline EPSC was not altered (Fig. S3), and complementary changes in the number of docking sites and their baseline occupancy were observed in Syt7 KD synapses (**Fig. 6** ☒). These results raise a possibility that Syt7 may play a role in providing additional vacant docking sites that can be overfilled during facilitation. It remains to be elucidated whether the decrease in the number of docking sites at Syt7 KD synapses is related to the subcellular localization of Syt7 to the plasma membrane of the active zone (Sugita et al., 2001 ☒; Vevea et al., 2021 ☒).

STP model in light of known Ca^{2+} binding kinetics of Syt7

Syt7 acts as an upstream Ca^{2+} sensor that facilitates activity-dependent replenishment (Liu et al., 2014 ☒; Bacaj et al., 2015 ☒; Chen et al., 2017 ☒; Tawfik et al., 2021 ☒). The present study shows that EPSCs are mediated by TS vesicles both at rest and during activity-dependent facilitation. Releasable vesicles are homogeneous, and Syt7-dependent overfilling is responsible for the activity-dependent enhancement of EPSCs. Thus, we tested whether slowly developing facilitation could be replicated within the framework of a simple refilling model based on the known Ca^{2+} binding kinetics of Syt7 (Brandt et al., 2012 ☒). To this end, we made following assumptions: (1) a Ca^{2+}-dependent increase in the forward refilling rate (k_1) requires a full Ca^{2+}-bound form of Syt7, to which multiple Ca^{2+} ions can bind (two or three Ca^{2+} ions on each C2A and/or C2B domain) (Brandt et al., 2012 ☒; Chon et al., 2015 ☒; Voleti et al., 2017 ☒); (2) sequential Ca^{2+} binding steps are synergistic through a cooperativity factor, b; (3) Syt7 senses AP-induced local $[Ca^{2+}]$ similar to that estimated at the calyx of Held (a Gaussian function with a full width at half maximum value of 0.2 ms and a peak of 40 μM) (Wang et al., 2008 ☒); and (4) residual $[Ca^{2+}]$ follows a mono-exponential function with an amplitude of 1 μM and decay time constant of 50 ms (Jackson and Redman, 2003 ☒).

Under these assumptions and the framework of the simple refilling model, slow and delayed facilitation could be replicated by modeling k_1 as $k_1 = k_{1,b} + K_{1,max} \times [Syt7: n\ Ca^{2+}]$, where $[Syt7: n\ Ca^{2+}]$ represents the fraction of fully Ca^{2+}-bound Syt7 (**Fig. 9A-C** ☒). Syt7 was slowly activated over the course of the stimulus train, suggesting that the cooperative binding of multiple Ca^{2+} ions progressively increased the putative active form of Syt7 because of its slow membrane binding/unbinding kinetics. Nevertheless, the late phase of facilitation at high frequencies was predicted to be higher in the simulation than in the experiment. As expected, based on the notion that sustained release during HFS is limited by site clearance in the active zone (**Fig. 4C** ☒), the model/data discrepancy became more pronounced at higher frequencies. Incorporating endocytic terms into the model may mitigate late-phase discrepancies.

Moreover, removal of the catalytic function of Syt7 in the model effectively accounted for the complete loss of facilitation observed in Syt7 KD (**Fig. 9D** ☒).
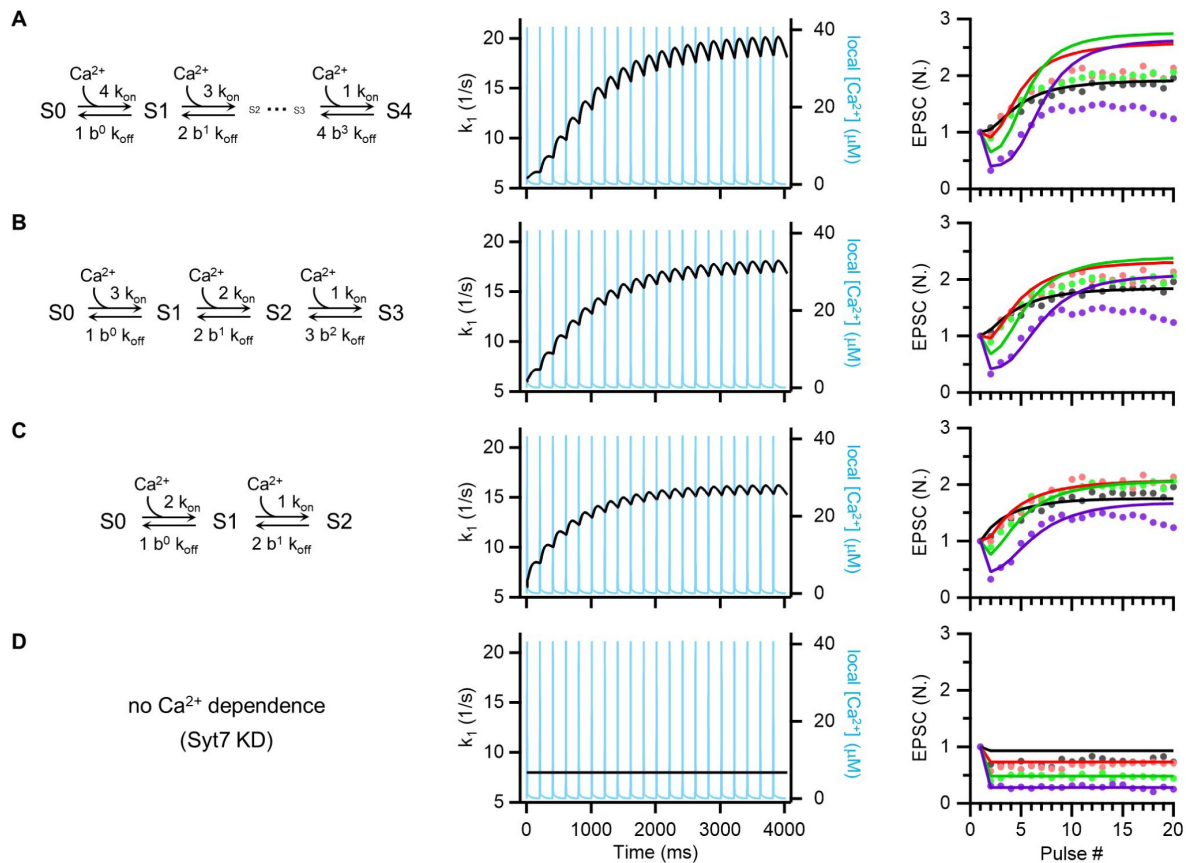
Figure 9.

STP model in light of known Ca^{2+} binding kinetics of Syt7

(**A-D**) *Left*, Schematic of allosteric calcium binding to Syt7. The number of Ca^{2+} bound to Syt7 was denoted as # in 'S#' in the reaction scheme. k_{on} = 7/μM/s, k_{off} = 10/s. *Middle*, Simulated changes of k_1 (*black*) in response to 5 Hz train of Ca^{2+} transients (*light blue traces*). The priming step of the simple refilling model was assumed to be catalyzed by full Ca^{2+}-bound from of Syt7. Accordingly, Ca^{2+}-dependent increase in k_1 was calculated as $K_{1,max}$ multiplied by a fraction of full Ca^{2+}-bound form of Syt7. We assumed that local $[Ca^{2+}]_i(t)$ follows a Gaussian function: $(1/\sigma \sqrt{2\pi}) \exp[-(t-t_p)^2/ 2\sigma^2]$, in which t_p = 0.25 ms and σ = 0.085 ms. *Right*, Fits of the Syt7 model to the STP data. To fit this model to the STP data, $K_{1,max}$ was set to 300/s (*A*), 220/s (*B*), and 180/s (*C*). Cooperativity factor (*b*) was set to 0.35 (*A*), 0.2 (*B*), and 0.05 (*C*). k_1 is set to be constant for Syt7 KD (*D*). Same frequency color codes were used as in **Figure 1** ☒.

Possible mechanisms underlying the depression-facilitation sequence

Cooperative binding of multiple Ca^{2+} ions to Syt7 predicts delayed activation and a progressive increase in vesicle refilling during train stimulations, resulting in delayed facilitation. Combining this with a high p_v could replicate not only the slow facilitation at 5 Hz, but also the unique depression-facilitation sequence observed at 40 Hz (**Fig. 9** ⧉). As simulated by Pulido and Marty (2018) ⧉, delayed facilitation can be reproduced by a high p_v in combination with a low baseline occupancy of replacement sites and subsequent Ca^{2+}-dependent refilling. However, whether this model is also able to replicate slow facilitation at low frequencies remains to be tested. An alternative, but not exclusive, possibility for delayed facilitation is that the presynaptic global Ca^{2+} itself may undergo a slow buildup during a train due to the saturation of endogenous Ca^{2+}-binding proteins.

Facilitation requires not only Syt7, but also activation of PLC-DAG signaling

To gain insight into the specific molecular mechanisms underlying the vesicle-loading processes, we examined the effects of pharmacological inhibitors targeting PLC and DAG (**Fig. 4** ⧉). Both a PLC inhibitor and a DAG analog reduced facilitation and augmentation. This suggests that the progressive overfilling of docking sites with TS vesicles is supported by the PLC-DAG signaling pathway and probably downstream Munc13 (Rhee et al., 2002 ⧉; Lou et al., 2008 ⧉). Phorbol esters have been recently shown to increase the TS fraction of docked vesicles by enhancing vesicle priming without affecting Ca^{2+} transients or p_v (Taschenberger et al., 2016 ⧉; Aldahabi et al., 2022 ⧉; Papantoniou et al., 2023 ⧉; Aldahabi et al., 2024 ⧉). In line with these findings, signaling involving PLC and DAG may support Ca^{2+}-dependent overfilling of TS vesicles by enhancing molecular priming processes.

Roles of facilitation and augmentation in working memory and related tasks

Previous theoretical studies have proposed that working memory in a recurrent network can be maintained in the form of augmentation at synapses (Mongillo et al., 2008 ⧉) and/or persistent activity of neurons in a memory ensemble. This is supported by the facilitation of recurrent excitatory synapses or disparity in STP between excitatory and inhibitory synapses. However, whether these short-term enhancements in synaptic efficacy contribute to working memory-related behaviors has not been examined. tFC is a temporal associative learning task requiring temporary retention of CS information during a trace period. The mPFC and hippocampus are crucial for tFC, and tFC is interfered with by a load of working memory and attention distraction, implying that the tFC shares the same neural substrate with other working memory tasks. In this study, tFC in WT and Syt7 KD animals revealed that Syt7 deficiency in the L2/3 pyramidal neurons of the mPFC impaired the acquisition of trace fear memory and reduced c-Fos expression associated with tFC training (**Fig. 8** ⧉). Given that synaptic enhancements in prelimbic L2/3 recurrent excitatory synapses can be attributed to an increase in p_{occ}, these behavioral results suggest that presynaptic high Ca^{2+} transients are temporally memorized in the presynaptic terminal as an increase in TS occupancy.

Conclusions

Progressive overfilling of synaptic vesicles with a high fusion probability supports the facilitation and augmentation of recurrent excitatory synapses within the L2/3 network of the mPFC and is essential for temporal associative learning.

Materials and methods

Animals/Subjects

All experiments were carried out on Sprague-Dawley rats of either sex at p28-43. Rats were maintained in temperature-controlled rooms on a constant 12 h light/12 h dark cycle and were given access to water and food ad libitum. All animal procedures were approved and performed in accordance with the Institutional Animal Care and Use Committee at Seoul National University (SNU200522-1).

In utero electroporation (IUE)

Pregnant Sprague Dawley rats on embryonic day (E) 17.5 were deeply anesthetized with 5% (v/v) isoflurane for the duration of surgery. The uterine horns were exposed by laparotomy and wet with warm sterile phosphate-buffered saline (PBS). The plasmids (0.5-2 µg/µl) together with the 0.01% fast green dye were injected into either the left or the right lateral ventricle or bilateral ventricles of embryos through a thin glass capillary (Narishige PC-10). The embryo's head was carefully held between the forceps-shaped electrodes of 10 mm diameter (CUY65010; NEPAGENE, Japan). Electroporation pulses (50 V for 50 ms) were delivered five times at intervals of 150 ms using a square-wave generator (ECM830; BEX, United States). The uterine horns were placed back into the abdominal cavity and abdominal muscles and skin were sutured. After the surgery, the animals were recovered under the infrared lamp. For knockdown experiments in slice electrophysiology, the shRNA constructs were co-electroporated with the pCAG-oChIEF-tdTomato, because of the consistent co-expression of the two constructs in a significant proportion of the transfected cells in vivo (Bony et al., 2013). Pups with robust fluorescence signals in the prefrontal cortex of both hemispheres were used for behavior experiments.

Preparation of vector constructs

For an optic stimulation, pCAG-oChIEF-tdTomato was transfected by IUE. Short hairpin RNA (shRNA) against Syt7 sequence (GATCTACCTGTCCTGGAAGAG) was expressed under the control of an U6 promoter of pAAV-U6-GFP vector (Cell Biolabs, #VPK-413). This shRNA was shown to effectively knockdown Syt7 in cell cultures and in vivo by previous reports from more than one research group (Bacaj et al., 2013 ; Li et al., 2017). Scrambled control sequence (TCGCATAGCGTATGCCGTT) was designed by shuffling the recognition region sequences and a BLAST analysis confirmed that the control shRNA sequence had no target gene. For rescue experiments, the cDNA for rat Syt7 (NM_021659) rendered resistant to the shRNA were inserted in the KD vector and their expression was driven by the CAG promoter; the vector also contained a self-cleaving P2A peptide sequence followed by EGFP, which ensures visualization of transfected cells. All the constructs above were verified by DNA sequencing. Plasmid DNA was purified and concentrated under endotoxin free conditions (Qiagen EndoFree Maxi Kit).

Slice preparation

Acute brain slices were prepared by using a VT1200S Vibratome (Leica Microsystems) after isoflurane anesthesia and decapitation. Coronal sections of the mPFC (300 µm in thickness) were cut in ice-cold artificial cerebrospinal fluid (aCSF) composed of (in mM) 125 NaCl, 3.2 KCl, 25 $NaHCO_3$, 1.25 NaH_2PO_4, 20 D-glucose, 2 NaPyr, 1 $MgCl_2$, and 1.3 $CaCl_2$ (Yoon et al., 2020), bubbled with 95% O_2 and CO_2 (pH = 7.3; 310 mOsm). Slices were allowed to recover for a minimum of 30 minutes at 36 °C, and subsequently maintained at room temperature until recording. Composition of aCSF was identical throughout the preparation, incubation, and

recording periods unless otherwise stated. For the recordings, the mPFC slices were continuously perfused with oxygenated aCSF at a flow rate of 1.5 ml/min, and the temperature was maintained at 31–32 °C using an in-line temperature controller (Warner Instruments).

Electrophysiology

Whole-cell patch-clamp recordings were performed from pyramidal cells and fast-spiking interneurons in layer 2/3 of the prelimbic mPFC. Neuronal subtypes were initially selected based on morphology under visual guidance by using an upright microscope equipped with infrared differential interference contrast (IR-DIC) optics (BX51WI, Olympus), and were further identified by their electrophysiological properties (see Supplementary Fig. 1; van Aerde and Feldmeyer, 2015 ; Tremblay et al., 2016). To analyze these intrinsic properties in current-clamp experiments, we measured the following parameters: (1) resting membrane potential (RMP), (2) input resistance (R_{in}), (3) sag ratio, and (4) the F-I curve, which plots firing frequencies (F) against the amplitude of injected currents (I). Both cell types exhibited a low sag ratio below 0.1, consistent with findings from other studies (van Aerde and Feldmeyer, 2015 ; Yoon et al., 2020). PCs and FSINs were easily distinguished by their unique firing frequency, Rin, spike adaptation, RMP and morphological characteristics including the shape of soma and the thickness of apical dendrites. For experiments involving oChIEF-expressing neurons in WT or Syt7 KD rats, whole-cell recordings were performed from the fluorescently labeled pyramidal neurons in layer 2/3 of the prelimbic cortex using suitable filter sets. Patch pipettes (tip resistance of 2–3 MΩ) were pulled from borosilicate glass and filled with (in mM) 130 K-gluconate, 8 KCl, 10 HEPES, 0.2 EGTA, 20 Na$_2$Pcr, 0.3 Na$_2$GTP, 4 MgATP. Intracellular solutions were adjusted to pH 7.25 and 300–310 mOsm. Neurons were voltage clamped at −78 mV and series resistance (Rs) were continuously monitored during the EPSCs recordings. Experiments were discarded before analysis if the Rs changed by 20% or larger deviation of baseline value. Measurements were not corrected for Rs compensation, bridge balance, or liquid junction potential. Electrophysiological data were low-pass-filtered at 1 kHz (Bessel) and acquired at 20 kHz using a Multiclamp 700B amplifier paired with Digidata 1440A digitizer and Clampex 10.2 software (Molecular Devices).

Synaptic stimulation

IUE resulted in sparse expression of channelrhodopsin (10-20%) (**Fig. 1A**). Exploiting the sparse expression, we employed a minimal optical stimulation method to activate a single or very few excitatory synapses in layer 2/3. The optic minimal stimulation was performed by our published protocol with minor modifications (Yoon et al., 2020). This approach aimed to minimize the risk of synaptic contamination, which could arise from engaging extra terminals that were initially inactive (depolarized below threshold) but became active by temporal summation during high-frequency trains. It also helped prevent the buildup of depolarization at the synaptic terminals, which might influence the probability of release, as noted by (Jackman et al., 2014). To achieve this, we employed a collimated digital micromirror device (DMD)-coupled LED (Polygon400; Mightex Systems) to confine 470 nm blue light to a small area with a radius of approximately 3–8 μm (typically 3–4 μm), as measured at the focal plane of a 60× water immersion objective [numerical aperture (NA) = 1.0; LUMPlanFL, Olympus] (Fig. S3A). To find the minimal stimulation area, the radius of illumination area was increased from 2 μm by 50% at each step (Fig. S3A), and selected the smallest illumination area that elicited EPSCs. Setting the duration of illumination between 3 and 5 ms (typically 5 ms), photostimulation onto oChIEF-expressing cells reliably induced action potentials (APs) during 600-pulse trains (see Fig. S2).

STP at various stimulus frequencies (5, 10, 20, and 40 Hz) was examined using 20-pulse trains. Trials of train stimulation were repeated with a prolonged interval of 30 s to avoid change in baseline properties. We observed no systematic changes in the amplitudes of the first EPSC of each train, nor did we find significant differences in the paired-pulse ratio (PPR) across stimulation trials in the same cell. For each stimulus frequency, approximately ten to twenty consecutive traces were collected and then averaged across trials to yield a mean EPSC trace. For recovery

experiments, two consecutive trains of 3 or 30 stimuli at 40 Hz, with varying time intervals (0.1-10 s), were applied every 10 s or 60 s, respectively, at both excitatory synapses. For 600-stimulus trains at 10Hz, the trial was delivered only once for each cell to avoid possible after-effects caused by prolonged synaptic stimulation (Hirsch and Crepel, 1990 ⧉). Prior to the stimulus trains, the EPSCs were normalized to the mean amplitude of the baseline. For the baseline measurements, paired pulses with various ISIs (20-200 ms) were delivered every 3 s (1/3 Hz) at least 20 times.

For all recordings, picrotoxin (PTX, 10 µM) was included in the recording solution to isolate glutamatergic responses. mPFC PC terminals were entirely glutamatergic as the application of 6-cyano-7-nitroquinoxaline-2,3-dione (CNQX, 20 µM), an AMPA receptor antagonist, completely abolished the monosynaptic events evoked by photostimulation. A low concentration of PTX was employed to minimize the relieving effects on spike suppression caused by blockade of GABAa receptors. We confirmed that no synaptic response was elicited by electrical stimulation in the presence of both 10 µM PTX and 20 µM CNQX.

In Fig. S4A, 1 µM TTX (1 mM stock solution) and 0.1 mM 4-AP (500 mM stock solution) were added to the bath solution to block action potentials and restore presynaptic glutamate release, respectively (Fig. S4A). In Fig. S5A, 50 µM of cyclothiazide, a positive allosteric modulator of the AMPA receptors, was included to minimize rapid desensitization of the postsynaptic receptors. In Fig. S5B, 0.5 mM kynurenate was added to bath solution to prevent possible saturation of AMPA receptors, especially during maximal synaptic facilitation. For pharmacological manipulations of synaptic vesicle dynamics (**Fig. 3** ⧉), drugs related to vesicle supply including U73122, OAG, LatB, EGTA-AM, and dynasore at indicated concentrations were added to the recording solution during baseline measurements or PTA/recovery experiments (IBI = 0.5 s). Chemicals were from Sigma-Aldrich, Merck, or Tocris.

Measurements of quantal size

Experiments for measuring asynchronous release were performed as previously described (Yoon et al., 2020 ⧉). In brief, we replaced extracellular Ca^{2+} entirely with 2 mM Sr^{2+} to induce asynchronous release. A single stimulus was delivered at 3-second intervals over 100 repetitions, and asynchronous release events were detected during a 100-ms window starting 25 ms after stimulus onset for each trial. The same procedure was also executed under sham conditions (0% light intensity) to serve as a control, thus mitigating contamination from nonspecific spontaneous events and potential errors associated with in the detection algorithm. q was determined as the mean value from the first Gaussian function after fitting the EPSC distribution with either a single or double Gaussian function (Fig. S8).

Calculation of probability for double failure

The failure rate at the 1st pulse when initial RRP size (n_1) = i can be calculated as: $P(F_1 \mid n_1=i) = (1 - p_v)^i$. The probability that initial RRP size is i was calculated as: $P(n_1=i) = C(N, i) * p^i * (1-p_{occ})^{(N-i)}$, where p_{occ} = mean release site occupancy, and N = total number of release sites. Under the conditions of no vesicle release at the 1st pulse (F_1) and $n_1 = i$, the probability for the second failure is

$$P(F_2 \mid n_1=i, F_1) = \sum_{n2=0..N} P(n_2 \mid n_1=i, F_1)\,(1 - p_v)^{n2}.$$

, where n_2 = number of vesicles just before the 2nd pulse. When forward and backward rate constants are k_1 and b_1, respectively, $P(n_2 \mid n_1=i, F1)$ is calculated as follows:

If $n_2 > i$, $P(n_2 \mid n_1=i, F1) = C(N-i, n_2-i)\,[1 - \exp(-k_1\,\Delta t)]^{(n2-i)}$.

If $n_2 < i$, $P(n_2 \mid n_1=i, F1) = C(i, i-n_2)\,[1 - \exp(-b_1\,\Delta t)]^{(i-n2)}$.

If $n_2 = i$, $P(n_2 \mid n_1=i, F1) = \exp[-i\,k1\,\Delta t]\,\exp[-i\,b_1\,\Delta t]$.

, where Δt = ISI. By the Bayes rule,

$$P(F_1, F_2, n_1=i) = P(F_2 \mid n_1=i, F_1) \, P(F_1 \mid n_1=i) \, P(n_1=i).$$

Thus, the probability for two consecutive failures can be calculated as:

$$P(F_1, F_2) = \Sigma_{i=0..N} \, P(F_2 \mid n_1 = i, F_1) \, P(F_1 \mid n_1=i) \, P(n_1=i).$$

$P(F_1)$ and N are observed values. The k_1 and p_v were set free variables. Other parameters were set according to following relationships: $P(F_1) = (1 - p_r)^N$, $p_r = p_v \, p_{occ}$, and $p_{occ} = k_1 / (k_1 + b_1)$.

Behavioral tests

Trace fear conditioning

For trace fear conditioning (tFC) (Gilmartin et al., 2013 ☐), individual rats were placed in the training chamber (30.5 x 25.4 x 30.5 cm; Coulbourn Instruments) consisting of metal grid floor connected to an electrical stimulator (H10-11R-TC-SF, Coulbourn Instruments) for delivery of a footshock. After a 5 min habituation period, rats received five pairings of a 20 s tone conditioned stimulus (CS, 2.5 kHz, 75 dB), followed by empty 20s trace period and a unconditioned stimulus (US; 1 s, 0.7 mA footshock) with a pseudorandom inter-trial interval (ITI) of 240 ± 20 s. During this training session, rats learned to associate the auditory CS with the shock US. The next day, the rats were tested for memory of CS-US trace association (called tone test). The acquisition of fear learning, often indicated by the extent of freezing to the CS, was assessed in a novel chamber (a white hexagonal enclosure) in a dimly lit room. During this tone (or retrieval) test, rats were first allowed to explore the new context for 5 min (habituation), followed by twelve 20 s CS presentations with a variable ITI of 120 ± 20 s. This entire session was repeated on the next day for assessment of extinction learning. Identities of the chambers were also determined with the presence of distinct odors; the training and testing chambers were cleaned with 70% ethanol and 1% acetic acid respectively before and after each session. For all experimental sessions, the activity of animals in the chambers was recorded at 30 frames per second using the EthoVision XT (Noldus Information Technology, Wageningen, Netherlands), and stored as a video file. The freezing behavior, defined as behavioral immobility other than respiratory movement, was assessed using an open-source video analysis pipeline ezTrack (Pennington et al., 2019 ☐). The percentage of freezing was calculated as a total duration of freezing divided by the total duration of observation.

Elevated Plus Maze

Elevated plus maze (EPM) test was performed using a plus-shaped apparatus elevated 60 cm above the ground. The maze consisted of two open arms (50 x 10 x 0.5 cm (H)), two closed arms (50 x 10 x 40 cm (H)) and a center area (10 x 10 cm). Rats were individually placed on the center area, facing an open arm, and the path of the animal was recorded with a video camera for 5 min. We analyzed the total distance traveled for 5 min and time spent in each arm. Animals were tracked offline using the open-source tracking system ezTrack (Pennington et al., 2019 ☐).

Open field test

Open field exploration test (OFT) was performed in an open field apparatus in a dimly lit room. The open field consisted of a white plastic board (1.20 m in diameter) surrounded by white plastic walls (50 cm in height). Individual rats were placed in a center zone (0.6 m in diameter), and allowed to freely explore the apparatus for 10 min. Time spent in the center zone and total distance traveled were analyzed for initial 5 min. Animals were tracked offline using the open-source tracking system ezTrack (Pennington et al., 2019 ☐).

Histology and immunohistochemistry

At the end of the behavioral experiments, rats were anesthetized using isoflurane inhalation and transcardially perfused with PBS followed by 4% paraformaldehyde (PFA, T&I, Korea). Brains were extracted and post-fixed in 4% PFA solution for 24 h. Perfused brains were sliced at 100 μM for estimation of GFP expression or 50 μM for immunohistochemistry. For analysis of c-Fos expression, rats were returned to their home cages immediately after the training session and perfused approximately 90 minutes later (Arime and Akiyama, 2017 ⧉). Brains were then cryopreserved, frozen, and sectioned coronally. Immunofluorescence staining was conducted on free-floating slices using a rabbit monoclonal anti c-fos (1:1000, Cell Signaling Technology, cat# 2250s) and mouse monoclonal anti-GAD67 (1:500, Millipore, cat# mab5406). Fluorescent secondary antibodies included Cy5-conjugated goat anti-rabbit IgG (1:1000, Abcam, cat# ab97077) and Cy3-conjugated goat anti-mouse IgG (1:1000, Abcam, cat# ab97035). Brain slices were permeabilized and blocked with PBS containing 0.5% Triton X-100 and 5% normal goat serum (NGS) for 1h at room temperature. Slices were incubated overnight at 4 °C with primary antibodies, followed by 4 h incubation with secondary antibodies at room temperature. Slices were then mounted with Antifading Mounting medium (Abcam, cat# ab104139). Confocal images were acquired using a Leica TCS SP8 microscope set to the same laser intensity and acquisition parameters to compare the immunosignals in sections from Scr and Syt7 KD groups. For cell counting and colocalization, fluorescent protein-positive cells were automatically quantified with spot-detection algorithms in Imaris 9.5 (Oxford instruments).

Data analysis

Data were analyzed and presented using ClampFit (Molecular Devices), Igor Pro (Wavemetrics), MATLAB (Mathworks), and Prism (GraphPad). Data points and error bars represent the mean ± standard error of the mean. All statistical analyses were conducted using two-tailed comparisons. Sample sizes and statistical tests for each group are detailed in the figure legends.

Numerical integration of the simple refilling model

This model posits reversible docking of vesicles at finite release sites (N_{max}) with forward (k_1) and reverse rate constants (b_1) (Hosoi et al., 2007 ⧉; Neher and Sakaba, 2008 ⧉).

$$\underset{b_1}{\overset{k_1}{\rightleftarrows}} n \overset{p_v}{\rightarrow}$$

According to this scheme, $dn/dt = k_1 u - b_1 n - p_v n \delta(t - t_{AP})$, where u is the number of unoccupied sites (= $N_{max} - n$); t_{AP} is the timing of AP firing; and δ is the Dirac delta function. The p_v was assumed to be unity (Fig. S8). The sum of basal k_1 (= $k_{1,b}$) and b_1 was be estimated as 23/s from the dependence PPR on ISIs (Fig. S8Ab). From the baseline occupancy of 0.3 and $p_{occ} = k_1 / (k_1 + b_1)$, we could estimate baseline k_1 ($k_{1,b}$) and b_1 as 6.9/s, and 16.1/s, respectively. Ca^{2+} and Syt7-dependent increase of k was modeled as $k = k + K [Syt7: n\ Ca^{2+}]$, where $[Syt7: n\ Ca^{2+}]$ represents the fraction of full Ca^{2+}-bound Syt7. For deterministic simulations, we time-integrated a set of differential equations for each model using Euler methods with a time step of 1 ms. All calculations were performed on the platform of Matlab (R2022b, Mathworks, USA).

Acknowledgements

Additional information

Author contributions

All experiments were carried out at cell physiology lab under Y.K and S.H.L's supervision. Conception or design of the work: J.S. and S.H.L. Acquisition, analysis or interpretation of data for the work: J.S, Y.K. and L.S.H. Drafting the work or revising it critically for important intellectual content: J.S., S.Y.L, Y.K. and L.S.H.

Funding

References

Aldahabi M, Neher E, Nusser Z (2024) **Different states of synaptic vesicle priming explain target cell type-dependent differences in neurotransmitter release** *Proc Natl Acad Sci U S A* **121**

Aldahabi M, Balint F, Holderith N, Lorincz A, Reva M, Nusser Z (2022) **Different priming states of synaptic vesicles underlie distinct release probabilities at hippocampal excitatory synapses** *Neuron* **110**:4144–4161

Arime Y, Akiyama K (2017) **Abnormal neural activation patterns underlying working memory impairment in chronic phencyclidine-treated mice** *PLoS One* **12**

Bacaj T, Wu D, Burre J, Malenka RC, Liu X, Sudhof TC (2015) **Synaptotagmin-1 and -7 Are Redundantly Essential for Maintaining the Capacity of the Readily-Releasable Pool of Synaptic Vesicles** *PLoS Biol* **13**

Bacaj T, Wu D, Yang X, Morishita W, Zhou P, Xu W, Malenka RC, Sudhof TC (2013) **Synaptotagmin-1 and synaptotagmin-7 trigger synchronous and asynchronous phases of neurotransmitter release** *Neuron* **80**:947–959

Baeg EH, Kim YB, Huh K, Mook-Jung I, Kim HT, Jung MW (2003) **Dynamics of population code for working memory in the prefrontal cortex** *Neuron* **40**:177–188

Bony G, Szczurkowska J, Tamagno I, Shelly M, Contestabile A, Cancedda L (2013) **Non-hyperpolarizing GABAB receptor activation regulates neuronal migration and neurite growth and specification by cAMP/LKB1** *Nat Commun* **4**

Brandt DS, Coffman MD, Falke JJ, Knight JD (2012) **Hydrophobic contributions to the membrane docking of synaptotagmin 7 C2A domain: mechanistic contrast between isoforms 1 and 7** *Biochemistry* **51**:7654–7664

Chen C, Satterfield R, Young SM, Jonas P (2017) **Triple Function of Synaptotagmin 7 Ensures Efficiency of High-Frequency Transmission at Central GABAergic Synapses** *Cell Rep* **21**:2082–2089

Chon NL, Osterberg JR, Henderson J, Khan HM, Reuter N, Knight JD, Lin H (2015) **Membrane Docking of the Synaptotagmin 7 C2A Domain: Computation Reveals Interplay between Electrostatic and Hydrophobic Contributions** *Biochemistry* **54**:5696–5711

Dittman JS, Kreitzer AC, Regehr WG (2000) **Interplay between facilitation, depression, and residual calcium at three presynaptic terminals** *J Neurosci* **20**:1374–1385

Fields RD, Eshete F, Stevens B, Itoh K (1997) **Action potential-dependent regulation of gene expression: temporal specificity in ca2+, cAMP-responsive element binding proteins, and mitogen-activated protein kinase signaling** *J Neurosci* **17**:7252–7266

Fujisawa S, Amarasingham A, Harrison MT, Buzsaki G (2008) **Behavior-dependent short-term assembly dynamics in the medial prefrontal cortex** *Nat Neurosci* **11**:823–833

Gilmartin MR, Miyawaki H, Helmstetter FJ, Diba K (2013) **Prefrontal activity links nonoverlapping events in memory** *J Neurosci* **33**:10910–10914

Guzowski JF, Timlin JA, Roysam B, McNaughton BL, Worley PF, Barnes CA (2005) **Mapping behaviorally relevant neural circuits with immediate-early gene expression** *Curr Opin Neurobiol* **15**:599–606

Hallermann S, Silver RA (2013) **Sustaining rapid vesicular release at active zones: potential roles for vesicle tethering** *Trends Neurosci* **36**:185–194

Hansel D, Mato G (2013) **Short-term plasticity explains irregular persistent activity in working memory tasks** *J Neurosci* **33**:133–149

Hass CA, Glickfeld LL (2016) **High-fidelity optical excitation of cortico-cortical projections at physiological frequencies** *J Neurophysiol* **116**:2056–2066

Haucke V, Neher E, Sigrist SJ (2011) **Protein scaffolds in the coupling of synaptic exocytosis and endocytosis** *Nat Rev Neurosci* **12**:127–138

Hempel CM, Hartman KH, Wang XJ, Turrigiano GG, Nelson SB (2000) **Multiple forms of short-term plasticity at excitatory synapses in rat medial prefrontal cortex** *J Neurophysiol* **83**:3031–3041

Hirsch JC, Crepel F (1990) **Use-dependent changes in synaptic efficacy in rat prefrontal neurons in vitro** *J Physiol* **427**:31–49

Holler S, Kostinger G, Martin KAC, Schuhknecht GFP, Stratford KJ (2021) **Structure and function of a neocortical synapse** *Nature* **591**:111–116

Holmgren C, Harkany T, Svennenfors B, Zilberter Y (2003) **Pyramidal cell communication within local networks in layer 2/3 of rat neocortex** *J Physiol* **551**:139–153

Hosoi N, Sakaba T, Neher E (2007) **Quantitative analysis of calcium-dependent vesicle recruitment and its functional role at the calyx of Held synapse** *J Neurosci* **27**:14286–14298

Jackman SL, Regehr WG (2017) **The Mechanisms and Functions of Synaptic Facilitation** *Neuron* **94**:447–464

Jackman SL, Beneduce BM, Drew IR, Regehr WG (2014) **Achieving high-frequency optical control of synaptic transmission** *J Neurosci* **34**:7704–7714

Jackman SL, Turecek J, Belinsky JE, Regehr WG (2016) **The calcium sensor synaptotagmin 7 is required for synaptic facilitation** *Nature* **529**:88–91

Jackson MB, Redman SJ (2003) **Calcium dynamics, buffering, and buffer saturation in the boutons of dentate granule-cell axons in the hilus** *J Neurosci* **23**:1612–1621

Kobbersmed JRL, Grasskamp AT, Jusyte M, Böhme MA, Ditlevsen S, Sørensen JB, Walter AM (2020) **Rapid regulation of vesicle priming explains synaptic facilitation despite heterogeneous vesicle:Ca2+ channel distances** *eLife* **9**

Kusick GF, Chin M, Raychaudhuri S, Lippmann K, Adula KP, Hujber EJ, Vu T, Davis MW, Jorgensen EM, Watanabe S (2020) **Synaptic vesicles transiently dock to refill release sites** *Nat Neurosci* **23**:1329–1338

Lee HR, Choi SH, Lee SH (2024) **Differential involvement of mitochondria in post-tetanic potentiation at intracortical excitatory synapses of the medial prefrontal cortex** *Cereb Cortex* **34**

Lee JS, Ho WK, Lee SH (2010) **Post-tetanic increase in the fast-releasing synaptic vesicle pool at the expense of the slowly releasing pool** *J Gen Physiol* **136**:259–272

Lee JS, Ho WK, Lee SH (2012) **Actin-dependent rapid recruitment of reluctant synaptic vesicles into a fast-releasing vesicle pool** *Proc Natl Acad Sci U S A* **109**:E765–774

Li YC, Chanaday NL, Xu W, Kavalali ET (2017) **Synaptotagmin-1- and Synaptotagmin-7-Dependent Fusion Mechanisms Target Synaptic Vesicles to Kinetically Distinct Endocytic Pathways** *Neuron* **93**:616–631

Lin JY, Lin MZ, Steinbach P, Tsien RY (2009) **Characterization of engineered channelrhodopsin variants with improved properties and kinetics** *Biophys J* **96**:1803–1814

Lin KH, Taschenberger H, Neher E (2022) **A sequential two-step priming scheme reproduces diversity in synaptic strength and short-term plasticity** *Proc Natl Acad Sci U S A* **119**

Liu H, Bai H, Hui E, Yang L, Evans CS, Wang Z, Kwon SE, Chapman ER (2014) **Synaptotagmin 7 functions as a Ca2+-sensor for synaptic vesicle replenishment** *Elife* **3**

Lou X, Korogod N, Brose N, Schneggenburger R (2008) **Phorbol esters modulate spontaneous and Ca2+-evoked transmitter release via acting on both Munc13 and protein kinase C** *J Neurosci* **28**:8257–8267

Macia E, Ehrlich M, Massol R, Boucrot E, Brunner C, Kirchhausen T (2006) **Dynasore, a cell-permeable inhibitor of dynamin** *Dev Cell* **10**:839–850

Malagon G, Miki T, Tran V, Gomez LC, Marty A (2020) **Incomplete vesicular docking limits synaptic strength under high release probability conditions** *Elife* **9**

Markram H, Wang Y, Tsodyks M (1998) **Differential signaling via the same axon of neocortical pyramidal neurons** *Proc Natl Acad Sci U S A* **95**:5323–5328

Martinetti LE, Bonekamp KE, Autio DM, Kim HH, Crandall SR (2022) **Short-Term Facilitation of Long-Range Corticocortical Synapses Revealed by Selective Optical Stimulation** *Cereb Cortex* **32**:1932–1949

Miki T, Malagon G, Pulido C, Llano I, Neher E, Marty A (2016) **Actin- and Myosin-Dependent Vesicle Loading of Presynaptic Docking Sites Prior to Exocytosis** *Neuron* **91**:808–823

Mongillo G, Barak O, Tsodyks M (2008) **Synaptic theory of working memory** *Science* **319**:1543–1546

Mongillo G, Hansel D, van Vreeswijk C (2012) **Bistability and spatiotemporal irregularity in neuronal networks with nonlinear synaptic transmission** *Phys Rev Lett* **108**

Neher E (2010) **What is Rate-Limiting during Sustained Synaptic Activity: Vesicle Supply or the Availability of Release Sites** *Front Synaptic Neurosci* **2**

Neher E (2024) **Interpretation of presynaptic phenotypes of synaptic plasticity in terms of a two-step priming process** *J Gen Physiol* **156**

Neher E, Sakaba T (2008) **Multiple roles of calcium ions in the regulation of neurotransmitter release** *Neuron* **59**:861–872

Neher E, Brose N (2018) **Dynamically Primed Synaptic Vesicle States: Key to Understand Synaptic Short-Term Plasticity** *Neuron* **100**:1283–1291

Norman CA, Krishnakumar SS, Timofeeva Y, Volynski KE (2023) **The release of inhibition model reproduces kinetics and plasticity of neurotransmitter release in central synapses** *Commun Biol* **6**

Otsuka T, Kawaguchi Y (2009) **Cortical inhibitory cell types differentially form intralaminar and interlaminar subnetworks with excitatory neurons** *J Neurosci* **29**:10533–10540

Ozdemir AT, Lagler M, Lagoun S, Malagon-Vina H, Lasztoczi B, Klausberger T (2020) **Unexpected Rule-Changes in a Working Memory Task Shape the Firing of Histologically Identified Delay-Tuned Neurons in the Prefrontal Cortex** *Cell Rep* **30**:1613–1626

Pan B, Zucker RS (2009) **A general model of synaptic transmission and short-term plasticity** *Neuron* **62**:539–554

Papantoniou C *et al.* (2023) **Munc13- and SNAP25-dependent molecular bridges play a key role in synaptic vesicle priming** *Sci Adv* **9**

Pennington ZT, Dong Z, Feng Y, Vetere LM, Page-Harley L, Shuman T, Cai DJ (2019) **ezTrack: An open-source video analysis pipeline for the investigation of animal behavior** *Sci Rep* **9**

Pulido C, Marty A (2018) **A two-step docking site model predicting different short-term synaptic plasticity patterns** *J Gen Physiol* **150**:1107–1124

Reyes A, Sakmann B (1999) **Developmental switch in the short-term modification of unitary EPSPs evoked in layer 2/3 and layer 5 pyramidal neurons of rat neocortex** *J Neurosci* **19**:3827–3835

Rhee JS *et al.* (2002) **Beta phorbol ester- and diacylglycerol-induced augmentation of transmitter release is mediated by Munc13s and not by PKCs** *Cell* **108**:121–133

Ritzau-Jost A, Jablonski L, Viotti J, Lipstein N, Eilers J, Hallermann S (2018) **Apparent calcium dependence of vesicle recruitment** *J Physiol* **596**:4693–4707

Ritzau-Jost A, Delvendahl I, Rings A, Byczkowicz N, Harada H, Shigemoto R, Hirrlinger J, Eilers J, Hallermann S (2014) **Ultrafast action potentials mediate kilohertz signaling at a central synapse** *Neuron* **84**:152–163

Rozov A, Burnashev N, Sakmann B, Neher E (2001) **Transmitter release modulation by intracellular Ca2+ buffers in facilitating and depressing nerve terminals of pyramidal cells in layer 2/3 of the rat neocortex indicates a target cell-specific difference in presynaptic calcium dynamics** *J Physiol* **531**:807–826

Sakaba T, Neher E (2003) **Involvement of actin polymerization in vesicle recruitment at the calyx of Held synapse** *J Neurosci* **23**:837–846

Scheuss V, Schneggenburger R, Neher E (2002) **Separation of presynaptic and postsynaptic contributions to depression by covariance analysis of successive EPSCs at the calyx of Held synapse** *J Neurosci* **22**:728–739

Silva M, Tran V, Marty A (2021) **Calcium-dependent docking of synaptic vesicles** *Trends Neurosci* **44**:579–592

Silva M, Tran V, Marty A (2024) **A maximum of two readily releasable vesicles per docking site at a cerebellar single active zone synapse** *Elife* **12**

Sugita S, Han W, Butz S, Liu X, Fernandez-Chacon R, Lao Y, Sudhof TC (2001) **Synaptotagmin VII as a plasma membrane Ca(2+) sensor in exocytosis** *Neuron* **30**:459–473

Taschenberger H, Woehler A, Neher E (2016) **Superpriming of synaptic vesicles as a common basis for intersynapse variability and modulation of synaptic strength** *Proc Natl Acad Sci U S A* **113**:E4548–4557

Tawfik B, Martins JS, Houy S, Imig C, Pinheiro PS, Wojcik SM, Brose N, Cooper BH, Sorensen JB (2021) **Synaptotagmin-7 places dense-core vesicles at the cell membrane to promote Munc13-2- and Ca(2+)-dependent priming** *Elife* **10**

Tran V, Silva M, Marty A (2023) **Prioritized docking of synaptic vesicles provided by a rapid recycling pathway** *iScience* **26**

Tremblay R, Lee S, Rudy B (2016) **GABAergic Interneurons in the Neocortex: From Cellular Properties to Circuits** *Neuron* **91**:260–292

Turecek J, Jackman SL, Regehr WG (2016) **Synaptic Specializations Support Frequency-Independent Purkinje Cell Output from the Cerebellar Cortex** *Cell Rep* **17**:3256–3268

Turecek J, Jackman SL, Regehr WG (2017) **Synaptotagmin 7 confers frequency invariance onto specialized depressing synapses** *Nature* **551**:503–506

Valera AM, Doussau F, Poulain B, Barbour B, Isope P (2012) **Adaptation of granule cell to Purkinje cell synapses to high-frequency transmission** *J Neurosci* **32**:3267–3280

van Aerde KI, Feldmeyer D (2015) **Morphological and physiological characterization of pyramidal neuron subtypes in rat medial prefrontal cortex** *Cereb Cortex* **25**:788–805

Vandael D, Borges-Merjane C, Zhang X, Jonas P (2020) **Short-Term Plasticity at Hippocampal Mossy Fiber Synapses Is Induced by Natural Activity Patterns and Associated with Vesicle Pool Engram Formation** *Neuron* **107**:509–521

Vevea JD, Kusick GF, Courtney KC, Chen E, Watanabe S, Chapman ER (2021) **Synaptotagmin 7 is targeted to the axonal plasma membrane through gamma-secretase processing to promote synaptic vesicle docking in mouse hippocampal neurons** *Elife* **10**

Voleti R, Tomchick DR, Sudhof TC, Rizo J (2017) **Exceptionally tight membrane-binding may explain the key role of the synaptotagmin-7 C(2)A domain in asynchronous neurotransmitter release** *Proc Natl Acad Sci U S A* **114**:E8518–E8527

Wang LY, Neher E, Taschenberger H (2008) **Synaptic vesicles in mature calyx of Held synapses sense higher nanodomain calcium concentrations during action potential-evoked glutamate release** *J Neurosci* **28**:14450–14458

Wu LG, Chan CY (2022) **Multiple Roles of Actin in Exo- and Endocytosis** *Front Synaptic Neurosci* **14**

Yau JO, McNally GP (2023) **The Rescorla-Wagner model, prediction error, and fear learning** *Neurobiol Learn Mem* **203**

Yoon JY, Lee HR, Ho WK, Lee SH (2020) **Disparities in Short-Term Depression Among Prefrontal Cortex Synapses Sustain Persistent Activity in a Balanced Network** *Cereb Cortex* **30**:113–134

Zucker RS, Regehr WG (2002) **Short-term synaptic plasticity** *Annu Rev Physiol* **64**:355–405

Author information

Jiwoo Shin

Department of Brain and Cognitive Science, College of Natural Sciences, Seoul National University, Seoul, South Korea, Department of Physiology, Seoul National University College of Medicine, Seoul, South Korea
ORCID iD: 0009-0001-2580-0368

Seung Yeon Lee

Department of Physiology, Seoul National University College of Medicine, Seoul, South Korea
ORCID iD: 0009-0009-5199-7369

Yujin Kim

Department of Brain and Cognitive Science, College of Natural Sciences, Seoul National University, Seoul, South Korea, Department of Physiology, Seoul National University College of Medicine, Seoul, South Korea

For correspondence: kim.y@snu.ac.kr

Suk-Ho Lee

Department of Brain and Cognitive Science, College of Natural Sciences, Seoul National University, Seoul, South Korea, Department of Physiology, Seoul National University College of Medicine, Seoul, South Korea
ORCID iD: 0000-0003-4117-5619

For correspondence: leesukho@snu.ac.kr

Editors

Reviewer #1 (Public review):

Shin et al. conduct extensive electrophysiological and behavioral experiments to study the mechanisms of short-term synaptic plasticity at excitatory synapses in layer 2/3 of the rat

medial prefrontal cortex. The authors interestingly find that short-term facilitation is driven by progressive overfilling of the readily releasable pool, and that this process is mediated by phospholipase C/diacylglycerol signaling and synaptotagmin-7 (Syt7). Specifically, knockdown of Syt7 not only abolishes the refilling rate of vesicles with high fusion probability, but it also impairs the acquisition of trace fear memory.

Overall, the authors offer novel insight to the field of synaptic plasticity through well-designed experiments that incorporate a range of techniques.

https://doi.org/10.7554/eLife.102923.1.sa2

Reviewer #2 (Public review):

Summary:

Shin et al aim to identify in a very extensive piece of work a mechanism that contributes to dynamic regulation of synaptic output in the rat cortex at the second time scale. This mechanism is related to a new powerful model is well versed to test if the pool of SV ready for fusion is dynamically scaled to adjust supply demand aspects. The methods applied are state-of-the-art and both address quantitative aspects with high signal to noise. In addition, the authors examine both excitatory output onto glutamatergic and GABAergic neurons, which provides important information on how general the observed signals are in neural networks, The results are compellingly clear and show that pool regulation may be predominantly responsible. Their results suggests that a regulation of release probability, the alternative contender for regulation, is unlikely to be involved in the observed short term plasticity behavior (but see below). Besides providing a clear analysis pof the underlying physiology, they test two molecular contenders for the observed mechanism by showing that loss of Synaptotagmin7 function and the role of the Ca dependent phospholipase activity seems critical for the short term plasticity behavior. The authors go on to test the in vivo role of the mechanism by modulating Syt7 function and examining working memory tasks as well as overall changes in network activity using immediate early gene activity. Finally, they model their data, providing strong support for their interpretation of TS pool occupancy regulation.

Strengths:

This is a very thorough study, addressing the research question from many different angles and the experimental execution is superb. The impact of the work is high, as it applies recent models of short term plasticity behavior to in vivo circuits further providing insights how synapses provide dynamic control to enable working memory related behavior through nonpermanent changes in synaptic output.

Weaknesses:

While this work is carefully examined and the results are presented and discussed in a detailed manner, the reviewer is still not fully convinced that regulation of release provability is not a putative contributor to the observed behavior. No additional work is needed but in the moment I am not convinced that changes in release probability are not in play. One solution may be to extend the discussion of changes in rules probability as an alternative.

Fig 3 I am confused about the interpretation of the Mean Variance analysis outcome. Since the data points follow the curve during induction of short term plasticity, aren't these suggesting that release probability and not the pool size increases? Related, to measure the absolute release probability and failure rate using the optogenetic stimulation technique is

not trivial as the experimental paradigm bias the experiment to a given output strength, and therefore a change in release probability cannot be excluded.

Fig4B interprets the phorbol ester stimulation to be the result of pool overfilling, however, phorbol ester stimulation has also been shown to increase release probability without changing the size of the readily releasable pool. The high frequency of stimulation may occlude an increased paired pulse depression in presence of OAG, which others have interpreted in mammalian synapses as an increase in release probability.

The literature on Syt7 function is still quite controversial. An observation in the literature that loss of Syt7 function in the fly synapse leads to an increase of release probability. Thus the observed changes in short term plasticity characteristics in the Syt7 KD experiments may contain a release probability component. Can the authors really exclude this possibility? Figure 5 shows for the Syt7 KD group a very prominent depression of the EPSC/IPSC with the second stimulus, particularly for the short interpulse intervals, usually a strong sign of increased release probability, as lack of pool refilling can unlikely explain the strong drop in synaptic output.

https://doi.org/10.7554/eLife.102923.1.sa1

Reviewer #3 (Public review):

Summary:

The report by Shin, Lee, Kim, and Lee entitled "Progressive overfilling of readily releasable pool underlies short-term facilitation at recurrent excitatory synapses in layer 2/3 of the rat prefrontal cortex" describes electrophysiological experiments of short-term synaptic plasticity during repetitive presynaptic stimulation at synapses between layer 2/3 pyramidal neurons and nearby target neurons. Manipulations include pharmacological inhibition of PLC and actin polymerization, activation of DAG receptors, and shRNA knockdown of Syt7. The results are interpreted as support for the hypothesis that synaptic vesicle release sites are vacant most of the time at resting synapses (i.e., p_occ is low) and that facilitation (and augmentation) components of short-term enhancement are caused by an increase in occupancy, presumably because of acceleration of the transition from not-occupied to occupied. The report additionally describes behavioural experiments where trace fear conditioning is degraded by knocking down syt7 in the same synapses.

Strengths:

The strength of the study is in the new information about short-term plasticity at local synapses in layer 2/3, and the major disruption of a memory task after eliminating short-term enhancement at only 15% of excitatory synapses in a single layer of a small brain region. The local synapses in layer 2/3 were previously difficult to study, but the authors have overcome a number of challenges by combining channel rhodopsins with in vitro electroporation, which is an impressive technical advance.

Weaknesses:

The question of whether or not short-term enhancement causes an increase in p_occ (i.e., "readily releasable pool overfilling") is important because it cuts to the heart of the ongoing debate about how to model short term synaptic plasticity in general. However, my opinion is that, in their current form, the results do not constitute strong support for an increase in p_occ, even though this is presented as the main conclusion. Instead, there are at least two alternative explanations for the results that both seem more likely. Neither alternative is acknowledged in the present version of the report.

The evidence presented to support overfilling is essentially two-fold. The first is strong paired pulse depression of synaptic strength when the interval between action potentials is 20 or 25 ms, but not when the interval is 50 ms. Subsequent stimuli at frequencies between 5 and 40 Hz then drive enhancement. The second is the observation that a slow component of recovery from depression after trains of action potentials is unveiled after eliminating enhancement by knocking down syt7. Of the two, the second is predicted by essentially all models where enhancement mechanisms operate independently of release site depletion - i.e., transient increases in p_{occ}, p_v, or even N - so isn't the sort of support that would distinguish the hypothesis from alternatives (Garcia-Perez and Wesseling, 2008, https://doi .org/10.1152/jn.01348.2007).

Regarding the paired pulse depression: The authors ascribe this to depletion of a homogeneous population of release sites, all with similar p_v. However, the details fit better with the alternative hypothesis that the depression is instead caused by quickly reversing inactivation of Ca2+ channels near release sites, as proposed by Dobrunz and Stevens to explain a similar phenomenon at a different type of synapse (1997, PNAS, https://doi.org/10.1073/pnas.94.26.14843). The details that fit better with Ca2+ channel inactivation include the combination of the sigmoid time course of the recovery from depression (plotted backwards in Fig1G,I) and observations that EGTA (Fig2B) increases the paired-pulse depression seen after 25 ms intervals. That is, the authors ascribe the sigmoid recovery to a delay in the activation of the facilitation mechanism, but the increased paired pulse depression after loading EGTA indicates, instead, that the facilitation mechanism has already caused p_r to double within the first 25 ms (relative to the value if the facilitation mechanism was not active). Meanwhile, Ca2+ channel inactivation would be expected to cause a sigmoidal recovery of synaptic strength because of the sigmoidal relationship between Ca2+-influx and exocytosis (Dodge and Rahamimoff, 1967, https://doi.org/10.1113 /jphysiol.1967.sp008367).

The Ca2+-channel inactivation hypothesis could probably be ruled in or out with experiments analogous to the 1997 Dobrunz study, except after lowering extracellular Ca2+ to the point where synaptic transmission failures are frequent. However, a possible complication might be a large increase in facilitation in low Ca2+ (Fig2B of Stevens and Wesseling, 1999, https:// doi.org/10.1016/s0896-6273(00)80685-6).

On the other hand, even if the paired pulse depression is caused by depletion of release sites rather than Ca2+-channel inactivation, there does not seem to be any support for the critical assumption that all of the release sites have similar p_v. And indeed, there seems to be substantial emerging evidence from other studies for multiple types of release sites with 5 to 20-fold differences in p_v at a wide variety of synapse types (Maschi and Klyachko, eLife, 2020, https://doi.org/10.7554/elife.55210; Rodriguez Gotor et al, eLife, 2024, https://doi.org/10 .7554/elife.88212 and refs. therein). If so, the paired pulse depression could be caused by depletion of release sites with high p_v, whereas the facilitation could occur at sites with much lower p_v that are still occupied. It might be possible to address this by eliminating assumptions about the distribution of p_v across release sites from the variance-mean analysis, but this seems difficult; simply showing how a few selected distributions wouldn't work - such as in standard multiple probability fluctuation analyses - wouldn't add much.

In any case, the large increase - often 10-fold or more - in enhancement seen after lowering Ca2+ below 0.25 mM at a broad range of synapses and neuro-muscular junctions noted above is a potent reason to be cautious about the LS/TS model. There is morphological evidence that the transitions from a loose to tight docking state (LS to TS) occur, and even that the timing is accelerated by activity. However, 10-fold enhancement would imply that at least 90 % of vesicles start off in the LS state, and this has not been reported. In addition, my understanding is that the reverse transition (TS to LS) is thought to occur within 10s of ms of

the action potential, which is 10-fold too fast to account for the reversal of facilitation seen at the same synapses (Kusick et al, 2020, https://doi.org/10.1038/s41593-020-00716-1).

Individual points:

(1) An additional problem with the overfilling hypothesis is that syt7 knockdown increases the estimate of p_occ extracted from the variance-mean analysis, which would imply a faster transition from unoccupied to occupied, and would consequently predict faster recovery from depression. However, recovery from depression seen in experiments was slower, not faster. Meanwhile, the apparent decrease in the estimate of N extracted from the mean-variance analysis is not anticipated by the authors' model, but fits well with alternatives where p_v varies extensively among release sites because release sites with low p_v would essentially be silent in the absence of facilitation.

(2) Figure S4A: I like the TTX part of this control, but the 4-AP part needs a positive control to be meaningful (e.g., absence of TTX).

(3) Line 251: At least some of the previous studies that concluded these drugs affect vesicle dynamics used logic that was based on some of the same assumptions that are problematic for the present study, so the reasoning is a bit circular.

(4) Line 329 and Line 461: A similar problem with circularity for interpreting earlier syt7 studies.

https://doi.org/10.7554/eLife.102923.1.sa0

Author Response:

We greatly appreciate invaluable and constructive comments from Editors and Reviewers. We also thank for their time and patience. We are pleased for our manuscript to have been assessed valuable and solid.

One of most critical concerns was a possible involvement of Ca2+ channel inactivation in the strong paired pulse depression (PPD). Meanwhile, we have already measured total (free plus buffered) calcium increments induced by each of first four APs in a 40 Hz train at axonal boutons of prelimbic layer 2/3 pyramidal cells. We found that first four Ca2+ increments were not different each other, arguing against possible contribution of Ca2+ channel inactivation to PPD. Please see our reply to the 2nd issue in the *Weakness* section of Reviewer #3.

The second critical issue was on the definition of 'vesicular probability'. Previously, vesicular probability (pv) has been used with reference to the releasable vesicle pool which includes not only tightly docked vesicles but also reluctant vesicles. On the other hand, the meaning of pv in the present study was release probability of tightly docked vesicles. We clarified this point in our replies to the 1st issues in the *Weakness* sections of Reviewer #2 and Reviewer #3.

To other Reviews' comments, we below described our point-by-point replies.

> **Reviewer #2 (Public review):**
>
> *Summary:*
>
> *Shin et al aim to identify in a very extensive piece of work a mechanism that contributes to dynamic regulation of synaptic output in the rat cortex at the second time scale. This mechanism is related to a new powerful model is well versed to test if the pool of SV ready for fusion is dynamically scaled to adjust supply demand aspects. The methods applied are state-of-the-art and both address quantitative aspects with high signal to noise. In addition, the authors examine both excitatory output onto glutamatergic and*

GABAergic neurons, which provides important information on how general the observed signals are in neural networks, The results are compellingly clear and show that pool regulation may be predominantly responsible. Their results suggests that a regulation of release probability, the alternative contender for regulation, is unlikely to be involved in the observed short term plasticity behavior (but see below). Besides providing a clear analysis pof the underlying physiology, they test two molecular contenders for the observed mechanism by showing that loss of Synaptotagmin7 function and the role of the Ca dependent phospholipase activity seems critical for the short term plasticity behavior. The authors go on to test the in vivo role of the mechanism by modulating Syt7 function and examining working memory tasks as well as overall changes in network activity using immediate early gene activity. Finally, they model their data, providing strong support for their interpretation of TS pool occupancy regulation.

Strengths:

This is a very thorough study, addressing the research question from many different angles and the experimental execution is superb. The impact of the work is high, as it applies recent models of short term plasticity behavior to in vivo circuits further providing insights how synapses provide dynamic control to enable working memory related behavior through nonpermanent changes in synaptic output.

Weaknesses:

While this work is carefully examined and the results are presented and discussed in a detailed manner, the reviewer is still not fully convinced that regulation of release provability is not a putative contributor to the observed behavior. No additional work is needed but in the moment I am not convinced that changes in release probability are not in play. One solution may be to extend the discussion of changes in rules probability as an alternative.

Quantal content (m) depends on n * pv, where n = RRP size and pv = vesicular release probability. The value for pv critically depends on the definition of RRP size. Recent studies revealed that docked vesicles have differential priming states: loosely or tightly docked state (LS or TS, respectively). Because the RRP size estimated by hypertonic solution or long presynaptic depolarization is larger than that by back extrapolation of a cumulative EPSC plot (Moulder & Mennerick, 2005; Sakaba, 2006) in glutamatergic synapses, the former RRP (denoted as RRPhyper) may encompass not only AP-evoked fast-releasing vesicles (TS vesicle) but also reluctant vesicles (LS vesicles). Because we measured pv based on AP-evoked EPSCs such as strong paired pulse depression (PPD) and associated failure rates, pv in the present study denotes vesicular fusion probability of TS vesicles not that of LS plus TS vesicles.

Recent studies suggest that release sites are not fully occupied by TS vesicles in the baseline (Miki et al., 2016; Pulido and Marty, 2018; Malagon et al., 2020; Lin et al., 2022). Instead the occupancy (pocc) by TS vesicles is subject to dynamic regulation by reversible rate constants (denoted by k1 and b1, respectively). The number of TS vesicles (n) can be factored into the number of release sites (N) and pocc, among which N is a fixed parameter but pocc depends on k1/(k1+b1) under the framework of the simple refilling model (see Methods). Because these refilling rate constants are regulated by Ca2+ (Hosoi, et al., 2008), pocc is not a fixed parameter. Therefore, release probability should be re-defined as pocc x pv. In this regard, the increase in release probability is a major player in STF. Our study asserts that STF by 2.3 times can be attributed to an increase in pocc rather than pv, because pv is close to unity (Fig. S8). Moreover, strong PPD was observed not only in the baseline but also at the early and in the middle of a train (Fig. 2 and 7) and during the recovery phase (Fig. 3), arguing against a gradual increase in pv of reluctant vesicles.

If the Reviewer meant vesicular release or fusion probability (pv) by 'release provability', pv (of TS vesicles) is not a major player in STF, because the baseline pv is already higher than 0.8 even if it is most parsimoniously estimated (Fig. 2). Moreover, considering very high refilling rate (23/s), the high double failure rate cannot be explained without assuming that pv is close to unity (Fig. S8).

Conventional models for facilitation assume a post-AP residual Ca^{2+}-dependent step increase in pv of RRP (Dittman et al., 2000) or reluctant vesicles (Turecek et al., 2016). Given that pv of TS vesicles is close to one, an increase in pv of TS vesicles cannot account for facilitation. The possibility for activity-dependent increase in fusion probability of LS vesicles (denoted as pv,LS) should be considered in two ways depending on whether LS and TS vesicles reside in distinct pools or in the same pool. Notably, strong PPD at short ISI implies that pv,LS is near zero at the resting state. Whereas LS vesicles do not contribute to baseline transmission, short-term facilitation (STF) may be mediated by cumulative increase in pv, LS that reside in a distinct pool. Because the increase in pv,LS during facilitation recruits new release sites (increase in N), the variance of EPSCs should become larger as stimulation frequency increases, resulting in upward deviation from a parabola in the V-M plane, as shown in recent studies (Valera et al., 2012; Kobbersmed et al., 2020). This prediction is not compatible with our results of V-M analysis (Fig. 3), showing that EPSCs during STF fell on the same parabola regardless of stimulation frequencies. Therefore, it is unlikely that an increase in fusion probability of reluctant vesicles residing in a distinct release pool mediates STF in the present study.

For the latter case, in which LS and TS vesicles occupy in the same release sites, it is hard to distinguish a step increase in fusion probability of LS vesicles from a conversion of LS vesicles to TS. Nevertheless, our results do not support the possibility for gradual increase in pv,LS that occurs in parallel with STF. Strong PPD, indicative of high pv, was consistently found not only in the baseline (Fig. 2 and Fig. S6) but also during post-tetanic augmentation phase (Fig. 3D) and even during the early development of facilitation (Fig. 2D-E and Fig. 7), arguing against gradual increase in pv,LS. One may argue that STF may be mediated by a drastic step increase of pv,LS from zero to one, but it is not distinguishable from conversion of LS to TS vesicles.

To address the reviewer's concern, we will incorporate these perspectives into the discussion and further clarify the reasoning behind our conclusions.

Moulder KL, Mennerick S (2005) Reluctant vesicles contribute to the total readily releasable pool in glutamatergic hippocampal neurons. J Neurosci 25:3842–3850.

Sakaba, T (2006) Roles of the fast-releasing and the slowly releasing vesicles in synaptic transmission at the calyx of Held. J Neurosci 26(22): 5863-5871.

> *Fig 3 I am confused about the interpretation of the Mean Variance analysis outcome. Since the data points follow the curve during induction of short term plasticity, aren't these suggesting that release probability and not the pool size increases? Related, to measure the absolute release probability and failure rate using the optogenetic stimulation technique is not trivial as the experimental paradigm bias the experiment to a given output strength, and therefore a change in release probability cannot be excluded.*

Under the recent definition of release probability, it can be factored into pv and pocc, which are fusion probability of TS vesicles and the occupancy of release sites by TS vesicles, respectively. With this regard, our interpretation of the Variance-Mean results is consistent with conventional one: different data points along a parabola represent a change in release

probability (= pocc x pv). Our novel finding is that the increase in release probability should be attributed to an increase in pocc, not to that in pv.

> *Fig4B interprets the phorbol ester stimulation to be the result of pool overfilling, however, phorbol ester stimulation has also been shown to increase release probability without changing the size of the readily releasable pool. The high frequency of stimulation may occlude an increased paired pulse depression in presence of OAG, which others have interpreted in mammalian synapses as an increase in release probability.*

To our experience in the calyx of Held synapses, OAG, a DAG analogue, increased the fast releasing vesicle pool (FRP) size (Lee JS et al., 2013), consistent with our interpretation (pool overfilling). Once the release sites are overfilled in the presence of OAG, it is expected that the maximal STF (ratio of facilitated to baseline EPSCs) becomes lower as long as the number of release sites (N) are limited. As aforementioned, the baseline pv is already close to one, and thus it cannot be further increased by OAG. Instead, the baseline pocc seems to be increased by OAG.

Lee JS, et al., Superpriming of synaptic vesicles after their recruitment to the readily releasable pool. Proc Natl Acad Sci U S A, 2013. 110(37): 15079-84.

> *The literature on Syt7 function is still quite controversial. An observation in the literature that loss of Syt7 function in the fly synapse leads to an increase of release probability. Thus the observed changes in short term plasticity characteristics in the Syt7 KD experiments may contain a release probability component. Can the authors really exclude this possibility? Figure 5 shows for the Syt7 KD group a very prominent depression of the EPSC/IPSC with the second stimulus, particularly for the short interpulse intervals, usually a strong sign of increased release probability, as lack of pool refilling can unlikely explain the strong drop in synaptic output.*

The reviewer raises an interesting point regarding the potential link between Syt7 KD and increased initial pv, particularly in light of observations in Drosophila synapses (Guan et al., 2020; Fujii et al., 2021), in which Syt7 mutants exhibited elevated initial pv. However, it is important to note that these findings markedly differ from those in mammalian systems, where the role of Syt7 in regulating initial pv has been extensively studied. In rodents, consistent evidence indicates that Syt7 does not significantly affect initial pv, as demonstrated in several studies (Jackman et al., 2016; Chen et al., 2017; Turecek and Regehr, 2018). Furthermore, in our study of excitatory synapses in the mPFC layer 2/3, we observed an initial pv already near its maximal level, approaching a value of 1. Consequently, it is unlikely that the loss of Syt7 could further elevate the initial pv. Instead, such effects are more plausibly explained by alternative mechanisms, such as alterations in vesicle replenishment dynamics, rather than a direct influence on pv.

Chen, C., et al., Triple Function of Synaptotagmin 7 Ensures Efficiency of High-Frequency Transmission at Central GABAergic Synapses. Cell Rep, 2017. 21(8): 2082-2089.

Fujii, T., et al., Synaptotagmin 7 switches short-term synaptic plasticity from depression to facilitation by suppressing synaptic transmission. Scientific reports, 2021. 11(1): 4059.

Guan, Z., et al., Drosophila Synaptotagmin 7 negatively regulates synaptic vesicle release and replenishment in a dosage-dependent manner. Elife, 2020. 9: e55443.

Jackman, S.L., et al., The calcium sensor synaptotagmin 7 is required for synaptic facilitation. Nature, 2016. 529(7584): 88-91.

Turecek, J. and W.G. Regehr, Synaptotagmin 7 mediates both facilitation and asynchronous release at granule cell synapses. Journal of Neuroscience, 2018. 38(13): 3240-3251.

Reviewer #3 (Public review):

Summary:

The report by Shin, Lee, Kim, and Lee entitled "Progressive overfilling of readily releasable pool underlies short-term facilitation at recurrent excitatory synapses in layer 2/3 of the rat prefrontal cortex" describes electrophysiological experiments of short-term synaptic plasticity during repetitive presynaptic stimulation at synapses between layer 2/3 pyramidal neurons and nearby target neurons. Manipulations include pharmacological inhibition of PLC and actin polymerization, activation of DAG receptors, and shRNA knockdown of Syt7. The results are interpreted as support for the hypothesis that synaptic vesicle release sites are vacant most of the time at resting synapses (i.e., p_occ is low) and that facilitation (and augmentation) components of short-term enhancement are caused by an increase in occupancy, presumably because of acceleration of the transition from not-occupied to occupied. The report additionally describes behavioural experiments where trace fear conditioning is degraded by knocking down syt7 in the same synapses.

Strengths:

The strength of the study is in the new information about short-term plasticity at local synapses in layer 2/3, and the major disruption of a memory task after eliminating short-term enhancement at only 15% of excitatory synapses in a single layer of a small brain region. The local synapses in layer 2/3 were previously difficult to study, but the authors have overcome a number of challenges by combining channel rhodopsins with in vitro electroporation, which is an impressive technical advance.

Weaknesses:

The question of whether or not short-term enhancement causes an increase in p_occ (i.e., "readily releasable pool overfilling") is important because it cuts to the heart of the ongoing debate about how to model short term synaptic plasticity in general. However, my opinion is that, in their current form, the results do not constitute strong support for an increase in p_occ, even though this is presented as the main conclusion. Instead, there are at least two alternative explanations for the results that both seem more likely. Neither alternative is acknowledged in the present version of the report.

The evidence presented to support overfilling is essentially two-fold. The first is strong paired pulse depression of synaptic strength when the interval between action potentials is 20 or 25 ms, but not when the interval is 50 ms. Subsequent stimuli at frequencies between 5 and 40 Hz then drive enhancement. The second is the observation that a slow component of recovery from depression after trains of action potentials is unveiled after eliminating enhancement by knocking down syt7. Of the two, the second is predicted by essentially all models where enhancement mechanisms operate independently of release site depletion - i.e., transient increases in p_occ, p_v, or even N - so isn't the sort of support that would distinguish the hypothesis from alternatives (Garcia-Perez and Wesseling, 2008, https://doi.org/10.1152/jn.01348.2007).

The apparent discrepancy in interpretation of post-tetanic augmentation between the present and previous papers [Sevens Wesseling (1999), Garcia-Perez and Wesseling (2008)] is an important issue that should be clarified. We noted that different meanings of 'vesicular release probability' in these papers are responsible for the discrepancy. We will add an explanation to Discussion on the difference in the meaning of 'vesicular release probability' between the present study and previous studies [Sevens Wesseling (1999), Garcia-Perez and Wesseling (2008)]. In summary, the pv in the present study was used for vesicular release

probability of TS vesicles, while previous studies used it as vesicular release probability of vesicles in the RRP, which include LS and TS vesicles. Accordingly, pocc in the present study is occupancy of release sites by TS vesicles.

Not only double failure rate but also other failure rates upon paired pulse stimulation were best fitted at pv close to 1 (Fig. S8 and associated text). Moreover, strong PPD, indicating release of vesicles with high pv, was observed not only at the beginning of a train but also in the middle of a 5 Hz train (Fig. 2D), during the augmentation phase after a 40 Hz train (Fig 3D), and in the recovery phase after three pulse bursts (Fig. 7). Given that pv is close to 1 throughout the EPSC trains and that N does not increase during a train (Fig. 3), synaptic facilitation can be attained only by the increase in pocc (occupancy of release sites by TS vesicles). In addition, it should be noted that Fig. 7 demonstrates strong PPD during the recovery phase after depletion of TS vesicles by three pulse bursts, indicating that recovered vesicles after depletion display high pv too. Knock-down of Syt7 slowed the recovery of TS vesicles after depletion of TS vesicles, highlighting that Syt7 accelerates the recovery of TS vesicles following their depletion.

As addressed in our reply to the first issue raised by Reviewer #2 and the third issue raised by Reviewer #3, our results do not support possibilities for recruitment of new release sites (increase in N) having low pv or for a gradual increase in pv of reluctant vesicles during short-term facilitation.

Previous studies suggested that an increase in pv is responsible for post-tetanic augmentation (Stevens and Wesseling, 1999; Garcia-Perez and Wesseling, 2008) by observing invariance of the RRP size after tetanic stimulation. In these studies, the RRP size was estimated by hypertonic sucrose solution or as the sum of EPSCs evoked 20 Hz/60 pulses train (denoted as 'RRPhyper'). Because reluctant vesicles (called LS vesicles) can be quickly converted to TS vesicles (16/s) and are released during a train (Lee et al., 2012), it is likely that the RRP size measured by these methods encompasses both LS and TS vesicles. In contrast, we assert high pv based on the observation of strong PPD and failure rates upon paired stimulations at ISI of 20 ms (Fig. 2 and Fig. S8). Given that single AP-induced vesicular release occurs from TS vesicles but not from LS vesicles, pv in the present study indicates the fusion probability of TS vesicles. From the same reasons, pocc denotes the occupancy of release sites by TS vesicles. Note that our study does not provide direct clue whether release sites are occupied by LS vesicles that are not tapped by a single AP, although an increase in the LS vesicle number may accelerate the recovery of TS vesicles. As suggested in Neher (2024), even if the number of LS plus TS vesicles are kept constant, an increase in pocc (occupancy by TS vesicles) would be interpreted as an increase in 'vesicular release probability' as in the previous studies (Stevens and Wesseling (1999); Garcia-Perez and Wesseling (2008)) as long as it was measured based on RRPhyper.

Regarding the paired pulse depression: The authors ascribe this to depletion of a homogeneous population of release sites, all with similar p_v. However, the details fit better with the alternative hypothesis that the depression is instead caused by quickly reversing inactivation of Ca2+ channels near release sites, as proposed by Dobrunz and Stevens to explain a similar phenomenon at a different type of synapse (1997, PNAS, https://doi.org/10.1073/pnas.94.26.14843). The details that fit better with Ca2+ channel inactivation include the combination of the sigmoid time course of the recovery from depression (plotted backwards in Fig1G,I) and observations that EGTA (Fig2B) increases the paired-pulse depression seen after 25 ms intervals. That is, the authors ascribe the sigmoid recovery to a delay in the activation of the facilitation mechanism, but the increased paired pulse depression after loading EGTA indicates, instead, that the facilitation mechanism has already caused p_r to double within the first 25 ms (relative to the value if the facilitation mechanism was not active). Meanwhile, Ca2+ channel inactivation would be expected to cause a sigmoidal recovery of synaptic strength
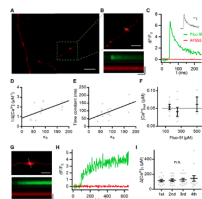
because of the sigmoidal relationship between Ca2+-influx and exocytosis (Dodge and Rahamimoff, 1967, https://doi.org/10.1113/jphysiol.1967.sp008367).

The Ca2+-channel inactivation hypothesis could probably be ruled in or out with experiments analogous to the 1997 Dobrunz study, except after lowering extracellular Ca2+ to the point where synaptic transmission failures are frequent. However, a possible complication might be a large increase in facilitation in low Ca2+ (Fig2B of Stevens and Wesseling, 1999, https://doi.org/10.1016/s0896-6273(00)80685-6).

We appreciate the reviewer's thoughtful comment regarding the potential role of Ca2+ channel inactivation in the observed paired-pulse depression (PPD). As noted by the Reviewer, the Dobrunz and Stevens (1997) suggested that the high double failure rate at short ISIs in synapses exhibiting PPD can be attributed to Ca2+ channel inactivation. This interpretation seems to be based on a premise that the number of RRP vesicles are not varied trial-by-trial. The number of TS vesicles, however, can be dynamically regulated depending on the parameters k1 and b1, as shown in Fig. S8, implying that the high double failure rate at short ISIs cannot be solely attributed to Ca2+ channel inactivation. Nevertheless, we acknowledge the possibility that Ca2+ channel inactivation may contribute to PPD, and therefore, we have further investigated this possibility. Specifically, we measured action potential (AP)-evoked Ca2+ transients at individual axonal boutons of layer 2/3 pyramidal cells in the mPFC using two-dye ratiometry techniques. Our analysis revealed no evidence for Ca2+ channel inactivation during a 40 Hz train of APs. This finding indicates that voltage-gated Ca2+ channel inactivation is unlikely to contribute to the pronounced PPD.

Author response image 1 below shows how we measured the total Ca2+ increments at axonal boutons. First we estimated endogenous Ca2+-binding ratio from analyses of single AP-induced Ca2+ transients at different concentrations of Ca2+ indicator dye (panels A to E). And then, using the Ca2+ buffer properties, we converted free [Ca2+] amplitudes to total calcium increments for the first four AP-evoked Ca2+ transients in a 40 Hz train (panels G-I). We will incorporate these results into the revised version of reviewed preprint to provide evidence against the Ca2+ channel inactivation.

Author response image 1.

On the other hand, even if the paired pulse depression is caused by depletion of release sites rather than Ca2+-channel inactivation, there does not seem to be any support for the critical assumption that all of the release sites have similar p_v. And indeed, there seems to be substantial emerging evidence from other studies for multiple types of release sites with 5 to 20-fold differences in p_v at a wide variety of synapse types (Maschi and Klyachko, eLife, 2020, https://doi.org/10.7554/elife.55210; Rodriguez Gotor et al, eLife, 2024, https://doi.org/10.7554/elife.88212 and refs. therein). If so, the paired pulse depression could be caused by depletion of release sites with high p_v, whereas the facilitation could occur at sites with much lower p_v that are still occupied. It might be possible to address this by eliminating assumptions about the distribution of p_v across release sites from the variance-mean analysis, but this seems difficult; simply showing

> *how a few selected distributions wouldn't work - such as in standard multiple probability fluctuation analyses - wouldn't add much.*

We appreciate the reviewer's insightful comments regarding the potential increase in pfusion of reluctant vesicles. It should be noted, however, that Maschi and Klyachko (2020) showed a distribution of release probability (pr) within a single active zone rather than a heterogeneity in pfusion of individual docked vesicles. Therefore both pocc and pv of TS vesicles would contribute to the pr distribution shown in Maschi and Klyachko (2020).

The Reviewer's concern aligns closely with the first issue raised by Reviewer #2, to which we addressed in detail. Briefly, new release site may not be recruited during facilitation or post-tetanic augmentation, because variance of EPSCs during and after a train fell on the same parabola (Fig. 3). Secondly, strong PPD was observed not only in the baseline but also during early and late phases of facilitation, indicating that vesicles with very high pv contribute to EPSC throughout train stimulations (Fig. 2, 3, and 7). These findings argue against the possibilities for recruitment of new release sites harboring low pv vesicles and for a gradual increase in fusion probability of reluctant vesicles.

To address the reviewers' concern, we will incorporate the perspectives into Discussion and further clarify the reasoning behind our conclusions.

> *In any case, the large increase - often 10-fold or more - in enhancement seen after lowering Ca2+ below 0.25 mM at a broad range of synapses and neuro-muscular junctions noted above is a potent reason to be cautious about the LS/TS model. There is morphological evidence that the transitions from a loose to tight docking state (LS to TS) occur, and even that the timing is accelerated by activity. However, 10-fold enhancement would imply that at least 90 % of vesicles start off in the LS state, and this has not been reported. In addition, my understanding is that the reverse transition (TS to LS) is thought to occur within 10s of ms of the action potential, which is 10-fold too fast to account for the reversal of facilitation seen at the same synapses (Kusick et al, 2020, https://doi.org/10.1038/s41593-020-00716-1).*

As the reviewer suggested, low external Ca2+ concentration can lower release probability (pr). Given that both pv and pocc are regulated by [Ca2+]i, low external [Ca2+] may affect not only pv but also pocc, both of which would contribute to low pr. Under such conditions, it would be plausible that the baseline pr becomes much lower than 0.1 due to low pv and pocc (for instance, pv decreases from 1 to 0.5, and pocc from 0.3 to 0.1, then pr = 0.05), and then pr (= pv x pocc) has a room for an increase by a factor of ten (0.5, for example) by short-term facilitation as cytosolic [Ca2+] accumulates during a train.

If pv is close to one, pr depends pocc, and thus facilitation depends on the number of TS vesicles just before arrival of each AP of a train. Thus, post-train recovery from facilitation would depend on restoration of equilibrium between TS and LS vesicles to the baseline. Even if transition between LS and TS vesicles is very fast (tens of ms), the equilibrium involved in *de novo* priming (reversible transitions between recycling vesicle pool and partially docked LS vesicles) seems to be much slower (13 s in Fig. 5A of Wu and Borst 1999). Thus, we can consider a two-step priming model (recycling pool -> LS -> TS), which is comprised of a slow 1st step (-> LS) and a fast 2nd step (-> TS). Under the framework of the two-step model, the slow 1st step (*de novo* priming step) is the rate limiting step regulating the development and recovery kinetics of facilitation. Given that on and off rate for Ca2+ binding to Syt7 is slow, it is plausible that Syt7 may contribute to short-term facilitation (STF) by Ca2+-dependent acceleration of the 1st step (as shown in Fig. 9). During train stimulation, the number of LS vesicles would slowly accumulate in a Syt7 and Ca2+-dependent manner, and this increase in LS vesicles would shift LS/TS equilibrium towards TS, resulting in STF. After tetanic

stimulation, the recovery kinetics from facilitation would be limited by slow recovery of LS vesicles.

Wu, L.-G. and Borst J.G.G. (1999) The reduced release probability of releasable vesicles during recovery from short-term synaptic depression. Neuron, 23(4): 821-832.

> *Individual points:*
>
> *(1) An additional problem with the overfilling hypothesis is that syt7 knockdown increases the estimate of p_occ extracted from the variance-mean analysis, which would imply a faster transition from unoccupied to occupied, and would consequently predict faster recovery from depression. However, recovery from depression seen in experiments was slower, not faster. Meanwhile, the apparent decrease in the estimate of N extracted from the mean-variance analysis is not anticipated by the authors' model, but fits well with alternatives where p_v varies extensively among release sites because release sites with low p_v would essentially be silent in the absence of facilitation.*

Slower recovery from depression observed in the Syt7 knockdown (KD) synapses (Fig. 7) may results from a deficiency in activity-dependent acceleration of TS vesicle recovery. Although basal occupancy was higher in the Syt7 KD synapses, this does not indicate a faster activity-dependent recovery.

Higher baseline occupancy does not always imply faster recovery of PPR too. Actually PPR recovery was slower in Syt7 KD synapses than WT one (18.5 vs. 23/s). Under the framework of the simple refilling model (Fig. S8Aa), the baseline occupancy and PPR recovery rate are calculated as $k1 / (k1 + b1)$ and $(k1 + b1)$, respectively. The baseline occupancy depends on $k1/b1$, while the PPR recovery on absolute values of $k1$ and $b1$. Based on pocc and PPR recovery time constant of WT and KD synapses, we expect higher $k1/b1$ but lower values for $(k1 + b1)$ in Syt7 KD synapses compared to WT ones.

Lower release sites (N) in Syt7-KD synapses was not anticipated. As you suggested, such low N might be ascribed to little recruitment of release sites during a train in KD synapses. But our results do not support this model. If silent release sites are recruited during a train, the variance should upwardly deviate from the parabola predicted under a fixed N (Valera et al., 2012; Kobbersmed et al. 2020). Our result was not the case (Fig. 3). In the first version of Ms, we have argued against this possibility in line 203-208.

As discussed in both the Results and Discussion sections, the baseline EPSC was unchanged by KD (Fig. S3) because of complementary changes in the number of docking sites and their baseline occupancy (Fig. 6). These findings suggest that Syt7 may be involved in maintaining additional vacant docking sites, which could be overfilled during facilitation. It remains to be determined whether the decrease in docking sites in Syt7 KD synapses is related to its specific localization of Syt7 at the plasma membrane of active zones, as proposed in previous studies (Sugita et al., 2001; Vevea et al., 2021).

> *(2) Figure S4A: I like the TTX part of this control, but the 4-AP part needs a positive control to be meaningful (e.g., absence of TTX).*

The reason why we used 4-AP in the presence of TTX was to increase the length constant of axon fibers and to facilitate the conduction of local depolarization in the illumination area to axon terminals. The lack of EPSC in the presence of 4-AP and TTX indicates that illumination area is distant from axon terminals enough for optic stimulation-induced local depolarization not to evoke synaptic transmission. This methodology has been employed in previous studies including the work of Little and Carter (2013).

Little JP and Carter AG (2013) Synaptic mechanisms underlying strong reciprocal connectivity between the medial prefrontal cortex and basolateral amygdala. J Neurosci, 33(39): 15333-15342.

> *(3) Line 251: At least some of the previous studies that concluded these drugs affect vesicle dynamics used logic that was based on some of the same assumptions that are problematic for the present study, so the reasoning is a bit circular.*
>
> *(4) Line 329 and Line 461: A similar problem with circularity for interpreting earlier syt7 studies.*

(Reply to #3 and #4) We selected the target molecules as candidates based on their well-characterized roles in vesicle dynamics, and aimed to investigate what aspects of STP are affected by these molecules in our experimental context. For example, we could find that the baseline pocc and short-term facilitation (STF) are enhanced by the baseline DAG level and train stimulation-induced PLC activation, respectively. Notably, the effect of dynasore informed us that slow site clearing is responsible for the late depression of 40 Hz train EPSC. The knock-down experiments also provided us with information on the critical role of Syt7 in replenishment of TS vesicles. These approaches do not deviate from standard scientific reasoning but rather builds upon prior knowledge to formulate and test hypotheses.

Importantly, our conclusions do not rely solely on the assumption that altering the target molecule impacts synaptic transmission. Instead, our conclusions are derived from a comprehensive analysis of diverse outcomes obtained through both pharmacological and genetic manipulations. These interpretations align closely with prior literature, further validating our conclusions.

Therefore, the use of established studies to guide candidate selection and the consistency of our findings with existing knowledge do not represent a logical circularity but rather a reinforcement of the proposed mechanism through converging lines of evidence.

https://doi.org/10.7554/eLife.102923.1.sa4